

Lellouch-Lüscher factor for the $K \rightarrow 3\pi$ decays

Jin-Yi Pang,¹ Rishabh Bubna,² Fabian Müller,² Akaki Rusetsky,^{2,3} and Jia-Jun Wu⁴

¹*College of Science, University of Shanghai for Science and Technology, Shanghai 200093, China*

²*Helmholtz-Institut für Strahlen- und Kernphysik (Theorie)*

and Bethe Center for Theoretical Physics, Universität Bonn, 53115 Bonn, Germany

³*Tbilisi State University, 0186 Tbilisi, Georgia*

⁴*School of Physical Sciences, University of Chinese Academy of Sciences, Beijing 100049, China*

E-mail: jypang@usst.edu.cn, bubna@hiskp.uni-bonn.de,

f.mueller@hiskp.uni-bonn.de, rusetsky@hiskp.uni-bonn.de,

wujiajun@ucas.ac.cn

ABSTRACT:

We derive an explicit expression for the Lellouch-Lüscher (LL) factor in the $K \rightarrow 3\pi$ decays at leading order (without derivative couplings). Several important technical details are addressed, like a proper decomposition into the isospin amplitudes, the choice of a minimal set of effective couplings and the renormalization, as well as the algorithm for the solution of the pertinent Faddeev equations in the infinite volume which is based on the contour deformation method. Most importantly, our numerical results demonstrate that the three-body force contributes very little to the LL factor. This result paves the way for the study of the $K \rightarrow 3\pi$ decays on the lattice.

Contents

1	Introduction	1
2	Derivation of the $K \rightarrow 3\pi$ LL formula	4
2.1	The Lagrangian in the three-particle picture	4
2.2	The Lagrangian in the particle-dimer picture	5
2.3	Matching in the two-body sector	6
2.4	Matching of the three-body and decay Lagrangians	8
2.5	Reduction of the redundant couplings	9
3	Faddeev equations and derivation of the LL factor	10
3.1	Faddeev equation for particle-dimer amplitude	10
3.2	Matching of the three-pion coupling	14
3.3	Derivation of the LL factor	16
4	Numerical calculation of LL factor	19
4.1	Solution of the Faddeev equation in the infinite volume	19
4.2	Finite-volume wave function	23
4.3	The LL factor	23
4.4	The Weak Hamiltonian	27
5	Conclusions	30
A	Integrating out the dimer fields	31
B	Three-pion amplitude in Chiral Perturbation Theory	32
C	Leading-order energy shift of the $n = 1$ state	34

1 Introduction

In the recent years, first results of the lattice studies of the spectrum in the three-particle systems have started to appear. These results have been analyzed by using three different but conceptually equivalent formalisms known as Relativistic Field Theory (RFT) [1, 2], Non-Relativistic Effective Field Theory (NREFT) [3, 4] and Finite-Volume Unitarity (FVU) [5, 6] approaches. The references to the activities in the field that include both formal developments as well as actual simulations on the lattice are collected here [1–65]. For more information on the subject, we refer the reader to the two recent reviews on the subject [66, 67].

One of the most intriguing and challenging tasks in the three-particle sector is the study of the three-particle decays. In this paper, we exclusively focus on the decays which proceed via the weak or electromagnetic forces – in other words, these particles would be absolutely stable in pure QCD. A classic example for this kind of decays is given by $K \rightarrow 3\pi$. Here, one could also count the decays that proceed via the isospin breaking (the most prominent example of this sort is given by the $\eta \rightarrow 3\pi$). Putting differently, the η is stable in pure *isospin-symmetric* QCD, with $m_u = m_d$, and the decay amplitude is proportional to the quark mass difference ($m_d - m_u$) (the higher-order terms in this small parameter will be neglected). A completely different picture emerges where both the formation and the decay of a particle (resonance) is caused by strong interactions which are described by the QCD Lagrangian alone. In this case, analytic continuation into the complex plane becomes inevitable. We shall not consider such processes in the present paper.

The main conceptual problem in the determination of the decay amplitudes on the lattice are caused by the presence of the final-state interactions. Since the mass of the decaying particle lies above the sum of the masses of the decay products, the propagators in the Feynman diagrams that describe final-state interaction may become singular in the integration region. This, at a fixed energy, leads to an irregular dependence of the measured matrix element on the lattice volume, rather than to the exponentially suppressed finite-volume corrections which emerge in the observables of stable particles. Lellouch and Lüscher [68] have shown that, in case of two-particle decays, this singular behavior is contained in a single function (the so-called LL factor), which relates the decay amplitudes in the infinite and in a finite volume. A crucial property of this function is that it depends on the dynamics in the final state (the two-body phase shifts, in this case¹), but not on the interactions that lead to the decay. Further development of these ideas can be found in Refs. [70–72] which include, in particular, the generalization to the moving frames and the multi-channel decays.

An analog of the LL formula for the three-particle decays has been derived only very recently, independently by two groups [58–60]. Albeit there is no substantial conceptual difference between the two- and three-particle cases (for example, the functions that describe an irregular volume-dependence also in the three-particle case depend solely on the parameters of the final-state interactions), an algebraic structure of the final expressions is much more cumbersome and obscure. In particular, there exists only one LL factor in the two-body decays, owing to the kinematic constraints (the magnitude of the relative momentum in the two-body decays is fixed by energy-momentum conservation). On the contrary, the three-body decays are characterized by an (infinite) tower of effective couplings that describe the dependence of the decay amplitudes on different kinematical invariants. Consequently, the LL factor is not a single function but a matrix, which should be truncated in actual calculations.

The aim of the present paper is to consider a single physical process, the kaon decay into three pions, and to work out the LL factor explicitly for this process in different isospin

¹In general, the LL factor receives contribution from an infinite tower of the partial waves, see, e.g., [69].

channels. In order to achieve this goal, the NREFT approach will be used. The choice of the process was not completely arbitrary – we believe that this will be one to be most likely studied decays in lattice QCD in the nearest future, not least since the three-pion decays of kaons are considered as one of the sources of information about CP violation in the light quark sector (see, e.g., [73]). Moreover, we believe that, taking into account the expected accuracy of lattice calculations at the present stage, in the beginning it will be reasonable to truncate all interactions in the two- and three-pion sectors at the lowest order, i.e., to consider only non-derivative couplings in the S-wave. These approximations will allow us to put the final result in a much more compact and transparent form, suitable for a direct use by lattice practitioners, even if the calculation of the most interesting CP -odd observables (for instance, the asymmetry of slopes in the decays of K^+ and K^- [74]) will, at the end, require the inclusion of the higher-order derivative couplings at the next-to-leading order.² Such a generalization can be however performed in a straightforward manner, using the methods described in the present paper.³ In order not to overload the presentation with the technical details, below we however do not discuss these higher-order terms at all.

Furthermore, there are several technical issues that were addressed only very briefly, or not addressed at all in the previous work on the problem that was carried out within the NREFT framework. Since the kaons can decay into different isospin channels, one has to explicitly write down the Faddeev equations in these channels.⁴ Moreover, as it is well known [80, 81], these Faddeev equations need to be renormalized. A choice of a minimal set of three-body couplings that suffices to render amplitudes cutoff-independent is rather non-trivial and will be discussed below. Moreover, we discuss an algorithm which will be used for a numerical solution of these Faddeev equations in the infinite volume. This algorithm is based on the deformation of the integration contour into the complex plane and has been known for a long time in the non-relativistic scattering theory. The discussion in case of relativistic kinematics in the literature is much more fragmented, and we shall attempt to fill this gap in the present paper.

The main objective of this paper is however not of a technical nature. Namely, we shall try to find an answer to the question, whether a prior knowledge of the exact values of the three-body couplings, which describe short-range three-body interactions, is essential for the determination of the LL factor. If the answer to this question were positive, it would substantially complicate the extraction of the decay amplitudes on the lattice. Indeed, for this, one would have to first accurately extract the three-pion couplings from the measured spectrum of three pions, which is quite a challenging task. Fortunately, it turns out that the LL factor shows very little dependence on the three-body force. For this reason, even a rough estimate of the three-body amplitude, based on Chiral Perturbation Theory (ChPT), will be sufficient for an accurate calculation of the LL factor which is essentially determined

²For more details on the counting scheme in the effective theory, we refer to [75, 76].

³The only (small) complication that may arise here is related to the emergent spurious poles in the two-body pion-pion scattering amplitude that could be however removed, using the method described in Refs. [77–79].

⁴Note that, in the RFT framework, the inclusion of the different isospin channels has been considered in Ref. [60].

through the S-wave $\pi\pi$ scattering lengths alone. This, in turn, paves the way for a direct extraction of the $K \rightarrow 3\pi$ amplitudes in lattice QCD, circumventing, at the initial stage, the determination of the three-pion couplings from the measured lattice spectrum.

The layout of the paper is the following. In Sect. 2 we write down the most general effective Lagrangian for the problem at hand (both in three-particle and particle-dimer picture). The matching between these alternative descriptions has been carried out, and an explicit expression for the LL factor in $K \rightarrow 3\pi$ decays is derived. In Sect. 3, the Faddeev equations in different isospin channels are explicitly written down and the renormalization issues are addressed. The matching to the relativistic amplitudes that will ultimately enable one to express the three-body couplings in the Lagrangian through the three-body amplitudes calculated in ChPT, is discussed. In Sect. 4, these Faddeev equations in the infinite volume are solved by using the contour rotation technique. Furthermore, the finite-volume energy spectrum of the three-pion system is obtained by solving the quantization condition and the finite-volume wave function are determined. All these are necessary ingredients for the calculation of the LL factor. We finally check the sensitivity of the calculated LL factor to the input values of the short-range part of the three-body threshold amplitude and find that in a wide interval, the LL factor practically does not depend on this input. Sect. 5 contains our conclusions.

2 Derivation of the $K \rightarrow 3\pi$ LL formula

2.1 The Lagrangian in the three-particle picture

In the following, we will consider the decay of a positively charged kaon K^+ into three pions, which is induced via weak interactions. There are two decay channels: $K^+ \rightarrow \pi^0\pi^0\pi^+$ and $K^+ \rightarrow \pi^+\pi^+\pi^-$. In order to describe the decay $K \rightarrow 3\pi$ within the NREFT approach, we adapt the Lagrangian given in [76], rewriting it in an arbitrary frame defined by the four-velocity v^μ :

$$\begin{aligned} \mathcal{L} = & \sum_{i_3} \pi_{i_3}^\dagger 2w_v (i(v\partial) - w_v) \pi_{i_3} + \mathcal{L}_2 + \mathcal{L}_3 \\ & + K_+^\dagger 2W_v (i(v\partial) - W_v) K_+ + \mathcal{L}_K, \end{aligned} \quad (2.1)$$

where $w_v = \sqrt{M_\pi^2 + \partial^2 - (v\partial)^2}$ and $W_v = \sqrt{M_K^2 + \partial^2 - (v\partial)^2}$ and M_π and M_K denote the masses of pions and kaons respectively. Note that we work in the basis with physical particles, so that the triplet of pion fields is given by $\pi_{i_3} = (\pi_+, \pi_0, \pi_-)$. At the leading order in the power counting the two-body Lagrangian reads as

$$\begin{aligned} \mathcal{L}_2 = & \frac{1}{2} C_1 \pi_0^\dagger \pi_0^\dagger \pi_0 \pi_0 + 2 C_2 \left(\pi_+^\dagger \pi_0^\dagger \pi_+ \pi_0 + \pi_-^\dagger \pi_0^\dagger \pi_- \pi_0 \right) + C_3 \left(\pi_+^\dagger \pi_-^\dagger \pi_0 \pi_0 + \text{h.c.} \right) \\ & + 2 C_4 \pi_+^\dagger \pi_-^\dagger \pi_+ \pi_- + \frac{1}{2} C_5 \left(\pi_+^\dagger \pi_+^\dagger \pi_+ \pi_+ + \pi_-^\dagger \pi_-^\dagger \pi_- \pi_- \right), \end{aligned} \quad (2.2)$$

while the three-body Lagrangian is given by

$$\mathcal{L}_3 = D_1 \left(\pi_+^\dagger \pi_+ + \pi_0^\dagger \pi_0 + \pi_-^\dagger \pi_- \right)^3$$

$$+ D_2 \left(2\pi_+^\dagger \pi_-^\dagger - \pi_0^\dagger \pi_0^\dagger \right) \left(\pi_+^\dagger \pi_+ + \pi_0^\dagger \pi_0 + \pi_-^\dagger \pi_- \right) \left(2\pi_+ \pi_- - \pi_0 \pi_0 \right). \quad (2.3)$$

The weak kaon decays are described by the Lagrangian

$$\mathcal{L}_K = G_1 \left(K_+^\dagger \pi_0 \pi_0 \pi_+ + \text{h.c.} \right) + G_2 \left(K_+^\dagger \pi_+ \pi_+ \pi_- + \text{h.c.} \right). \quad (2.4)$$

At higher orders, all Lagrangians are amended by the terms that contain space derivatives of all fields. A consistent power counting emerges, if one counts three-momenta as $\mathbf{p} = \mathcal{O}(\delta)$, where δ stands for a generic small parameter.⁵ Again, for consistency, one should count the difference $M_K - 3M_\pi$ as a quantity of order δ^2 [76]. As mentioned above, in this paper the higher-order terms in δ , corresponding to the derivative couplings, are not considered.

To summarize, the following couplings emerge at leading order in the three-particle picture:

- The couplings C_i , $i = 1, \dots, 5$, describing non-derivative pion-pion interactions in different isospin channels. These can be expressed through the S-wave $\pi\pi$ scattering lengths a_0, a_2 in a standard manner, through the matching condition.
- The three-body couplings in the pion system D_1, D_2 (the three-body force). On the lattice, they can be determined from the fit to the three-body spectrum.
- The couplings G_1, G_2 that describe the weak decays of charged kaons into three pions.

2.2 The Lagrangian in the particle-dimer picture

In the particle-dimer picture, the most general Lagrangian at the leading order reads as⁶

$$\begin{aligned} \tilde{\mathcal{L}} = & \sum_{i_3} \pi_{i_3}^\dagger 2w_v (i(v\partial) - w_v) \pi_{i_3} + \sum_{I, I_3} \sigma_I T_{II_3}^\dagger T_{II_3} + \tilde{\mathcal{L}}_2 + \tilde{\mathcal{L}}_3 \\ & + K_+^\dagger 2W_v (i(v\partial) - W_v) K_+ + \tilde{\mathcal{L}}_K, \end{aligned} \quad (2.5)$$

Here $\sigma_I = \pm 1$, depending on the sign of the two-body scattering length. Furthermore, $i_3 = -1, 0, 1$ and $I_3 = -I, \dots, I$ denote the isospin projection of the pions and isospin- I S-wave dimer field T_{II_3} , respectively. As two pions can couple to $I = 0, 1, 2$, all dimers with different isospins decouple and can be neglected. Furthermore, due to Bose-symmetry two pions can not be in an $I = 1$ state in the S-wave. Therefore, at the leading order, the $I = 1$ dimer does not contribute, and the two-body interaction is described by the Lagrangian

$$\tilde{\mathcal{L}}_2 = \sum_{I, I_3} \left(T_{II_3}^\dagger O_{II_3} + \text{h.c.} \right), \quad I = 0, 2, \quad (2.6)$$

where the dimer operator is given by a sum over two pion field operators with pertinent Clebsh-Gordan coefficients:

$$O_{II_3} = \sum_{i_3, i'_3} \frac{1}{2} f_I \langle 1, i_3; 1, i'_3 | I, I_3 \rangle \pi_{i_3} \pi_{i'_3}. \quad (2.7)$$

⁵In the manifestly covariant framework we are using here, one has $p_\perp^\mu \doteq p^\mu - v^\mu (v \cdot p) = \mathcal{O}(\delta)$ instead.

⁶More details about particle-dimer formalism can be found, e.g., in Refs. [4, 46, 59, 80–82].

Note also that $O_{1I_3} = 0$ for all $I_3 = -1, 0, 1$ follows due to Bose-symmetry. Furthermore, the couplings f_I describe the decay of a dimer into two pions and can be expressed through the S-wave $\pi\pi$ scattering lengths through the matching condition.

The construction of the three-body Lagrangian proceeds by defining particle-dimer operators in the channels with a different total isospin J :

$$\mathcal{O}_{J_3}^{(J,I)} = \sum_{I_3, i_3} \langle I, I_3; 1, i_3 | J, J_3 \rangle \pi_{i_3} T_{II_3}. \quad (2.8)$$

In the channels with the total isospin $J = 2$ and $J = 3$, there is only a single set of operators with the dimers having $I = 2$. For isospin $J = 1$, there are two independent operators, where the dimer has $I = 0$ and $I = 2$ respectively. The most general Lagrangian is thus given by:

$$\tilde{\mathcal{L}}_3 = \sum_{J, J_3} \sum_{I, I'} h_J^{(I, I')} \left(\mathcal{O}_{J_3}^{(J, I)} \right)^\dagger \mathcal{O}_{J_3}^{(J, I')}, \quad (2.9)$$

where, due to hermiticity, $h_J^{(I, I')} = h_J^{(I', I)}$ (Note that $h_J^{(I, I')}$ are real due to the T -invariance.). In the $J = 2$ and $J = 3$ channels, there is a single coupling, $h_2^{(2,2)}$ and $h_3^{(2,2)}$, respectively. For the channel with $J = 1$, there are three couplings $h_1^{(0,0)}$, $h_1^{(2,2)}$ and $h_1^{(2,0)} = h_1^{(0,2)}$.

Finally, $\tilde{\mathcal{L}}_K$ describes the weak kaon decay. Due to charge conservation, the positively charged kaon can only couple to the operators with $J_3 = 1$:

$$\tilde{\mathcal{L}}_K = \sum_{J, I} g^{(J, I)} \left(K_+^\dagger \mathcal{O}_1^{(J, I)} + \text{h.c.} \right). \quad (2.10)$$

Hence, in the particle-dimer picture, we have the following parameters in the lowest-order Lagrangian

- Two-particle-dimer couplings f_0, f_2 . These correspond to the couplings C_i in the three-particle picture.
- Three-body force in the particle-dimer picture, described by the couplings $h_1^{(0,0)}$, $h_1^{(2,2)}$, $h_1^{(2,0)}$, $h_2^{(2,2)}$ and $h_3^{(2,2)}$. These correspond to the couplings D_1, D_2 in the three-particle picture.
- The weak couplings $g^{(1,0)}, g^{(1,2)}, g^{(3,2)}$, corresponding to the parameters G_1, G_2 in the three-particle picture.

Despite the fact that the number of the couplings in different formalisms differ, these formalisms are equivalent. This equivalence is, however, a rather subtle issue, and is discussed in the remaining part of this section.

2.3 Matching in the two-body sector

The couplings f_I can be matched to the two-body S-wave scattering length in the $I = 0$ and $I = 2$ isospin channels. Due to isospin symmetry, the dimer propagator is diagonal in the isospin space:

$$i \langle 0 | T [T_{II_3}(x) T_{I'I'_3}^\dagger(y)] | 0 \rangle = \delta_{II'} \delta_{I_3 I'_3} \int \frac{d^4 P}{(2\pi)^4} e^{-iP(x-y)} S_I(P^2). \quad (2.11)$$



Figure 1. Full dimer propagator, obtained by summing up self-energy insertions to all orders. The blue double, gray double and black single lines denote the full dimer propagator, the free dimer propagator given by $-\sigma_I^{-1}\delta_{II'}\delta_{I_3I'_3}$, and the particle propagator. The blue dots represent the insertion of the vertex converting a dimer into particles.

Summing up the self-energy insertions (see Fig. 1), for $I = 0, 2$ we find

$$S_I(P^2) = \frac{f_I^{-2}}{-\sigma_I f_I^{-2} - \frac{1}{2}I(s)}, \quad s = P^2, \quad (2.12)$$

where, for $s \geq 4M_\pi^2$,

$$I(s) = \frac{\sigma(s)}{16\pi^2} \ln \frac{\sigma(s) - 1}{\sigma(s) + 1} = J(s) + \frac{i\sigma(s)}{16\pi}, \quad \sigma(s) = \left(1 - \frac{4M_\pi^2}{s + i\varepsilon}\right)^{1/2}, \quad (2.13)$$

while for $I = 1$ trivially $S_1(P^2) = -\sigma_1^{-1}$.

The two-particle scattering amplitude $\pi_{i'_3}(p_1) + \pi_{j'_3}(p_2) \rightarrow \pi_{i_3}(p_3) + \pi_{j_3}(p_4)$ is obtained from the dimer propagator by attaching the vertices that convert a dimer into a particle-pair. The isospin $I = 0, 2$ the amplitudes are given by:

$$T_I(p_1, p_2; p_3, p_4) = f_I^2 S_I(P^2) = \frac{16\pi\sqrt{s}}{16\pi\sqrt{s}[-\sigma_I f_I^{-2} - \frac{1}{2}J(s)] - ip(s)}, \quad (2.14)$$

where $P^2 = (p_1 + p_2)^2 = (p_3 + p_4)^2$ and $s = P^2 = 4(M_\pi^2 + p^2(s))$. Due to unitarity,

$$16\pi\sqrt{s}[-\sigma_I f_I^{-2} - \frac{1}{2}J(s)] = p(s) \cot \delta_I(s). \quad (2.15)$$

Therefore, for $I = 0, 2$, the matching to the scattering length a_I reads as:

$$\sigma_I^{-1} f_I^2 = 32\pi M_\pi a_I. \quad (2.16)$$

As discussed in appendix A, integrating out the dimer fields at tree level merely amounts to the replacement

$$T_{II_3} \rightarrow -\sigma_I^{-1} O_{II_3}. \quad (2.17)$$

The matching condition to the two-particle Lagrangian in the particle picture yields:

$$\begin{aligned} C_1 &= -\frac{1}{6} \left(\sigma_0^{-1} f_0^2 + 2\sigma_2^{-1} f_2^2 \right) = -16\pi M_\pi \frac{1}{3} (a_0 + 2a_2), \\ C_2 &= -\frac{1}{4} \sigma_2^{-1} f_2^2 = -16\pi M_\pi \frac{1}{2} a_2, \\ C_3 &= -\frac{1}{6} \left(\sigma_2^{-1} f_2^2 - \sigma_0^{-1} f_0^2 \right) = -16\pi M_\pi \frac{1}{3} (a_2 - a_0) \\ C_4 &= -\frac{1}{12} \left(2\sigma_0^{-1} f_0^2 + \sigma_2^{-1} f_2^2 \right) = -16\pi M_\pi \frac{1}{6} (2a_0 + a_2), \end{aligned}$$

$$C_5 = -\frac{1}{2} \sigma_2^{-1} f_2^2 = -16\pi M_\pi a_2. \quad (2.18)$$

This result agrees with [76].⁷

2.4 Matching of the three-body and decay Lagrangians

At tree level, carrying out the the replacement (2.17) in the particle-dimer operators, one straightforwardly gets:

$$\begin{aligned} \mathcal{O}_{J_3}^{(1,0)} &\rightarrow -\frac{\sigma_0^{-1} f_0}{2\sqrt{3}} (2\pi_+\pi_- - \pi_0\pi_0)\pi_{J_3}, \\ \mathcal{O}_{J_3}^{(1,2)} &\rightarrow -\frac{\sigma_2^{-1} f_2}{\sqrt{15}} (2\pi_+\pi_- - \pi_0\pi_0)\pi_{J_3}, \\ \mathcal{O}_{J_3}^{(2,2)} &\rightarrow 0, \\ \mathcal{O}_{\pm 3}^{(3,2)} &\rightarrow -\frac{\sigma_2^{-1} f_2}{2} \pi_\pm \pi_\pm \pi_\pm, \\ \mathcal{O}_{\pm 2}^{(3,2)} &\rightarrow -\frac{\sigma_2^{-1} f_2 \sqrt{3}}{2} \pi_\pm \pi_\pm \pi_0, \\ \mathcal{O}_{\pm 1}^{(3,2)} &\rightarrow -\frac{\sigma_2^{-1} f_2 \sqrt{3}}{2\sqrt{5}} (\pi_\pm \pi_\pm \pi_\mp + 2\pi_\pm \pi_0 \pi_0), \\ \mathcal{O}_0^{(3,2)} &\rightarrow -\frac{\sigma_2^{-1} f_2}{\sqrt{10}} (3\pi_+\pi_-\pi_0 + \pi_0\pi_0\pi_0). \end{aligned} \quad (2.19)$$

Furthermore, performing this replacement in the particle-dimer Lagrangian, one can identify the couplings D_1, D_2 from Eq. (2.3):

$$\begin{aligned} \sum_{J, J_3} \sum_{I, I'} h_J^{(I, I')} \left(\mathcal{O}_{J_3}^{(J, I)} \right)^\dagger \mathcal{O}_{J_3}^{(J, I')} &\rightarrow D_1 \left(\pi_+^\dagger \pi_+ + \pi_0^\dagger \pi_0 + \pi_-^\dagger \pi_- \right)^3 \\ &+ D_2 \left(2\pi_+^\dagger \pi_-^\dagger - \pi_0^\dagger \pi_0^\dagger \right) \left(\pi_+^\dagger \pi_+ + \pi_0^\dagger \pi_0 + \pi_-^\dagger \pi_- \right) \left(2\pi_+\pi_- - \pi_0\pi_0 \right), \end{aligned} \quad (2.20)$$

with

$$\begin{aligned} D_1 &= \frac{f_2^2}{4} h_3^{(2,2)}, \\ D_2 &= \frac{f_0^2}{12} h_1^{(0,0)} + \frac{\sigma_0^{-1} f_0 \sigma_2^{-1} f_2}{3\sqrt{5}} h_1^{(2,0)} + \frac{f_2^2}{15} h_1^{(2,2)} - \frac{3f_2^2}{20} h_3^{(2,2)}. \end{aligned} \quad (2.21)$$

Using the same replacement in the Lagrangian that describes the weak decays of kaons (2.4), one could read off the couplings G_1, G_2 :

$$\sum_{J, I} g^{(J, I)} \left(K_+^\dagger \mathcal{O}_1^{(J, I)} + \text{h.c.} \right) \rightarrow G_1 \left(K_+^\dagger \pi_+\pi_+\pi_- + \text{h.c.} \right) + G_2 \left(K_+^\dagger \pi_+\pi_0\pi_0 + \text{h.c.} \right), \quad (2.22)$$

with

$$G_1 = -\frac{\sqrt{3}}{\sqrt{5}} \sigma_2^{-1} f_2 g^{(3,2)} + \frac{1}{\sqrt{15}} \sigma_2^{-1} f_2 g^{(1,2)} + \frac{1}{2\sqrt{3}} \sigma_0^{-1} f_0 g^{(1,0)}.$$

⁷Note a different sign convention is used in Ref. [76], namely, $p \cot \delta = 1/a_I + \dots$ instead of $p \cot \delta = -1/a_I + \dots$

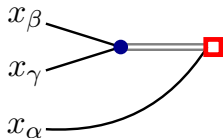


Figure 2. Tree level contribution to the decay matrix element. Black solid lines and gray double lines denote a particle propagator and the tree-level dimer propagator, respectively. The blue dot and the empty red square correspond to the particle-dimer conversion vertex and the kaon initial decay coupling, respectively. Furthermore, $(\alpha\beta\gamma)$ stands for some permutation of (123) .

$$G_2 = -\frac{\sqrt{3}}{2\sqrt{5}} \sigma_2^{-1} f_2 g^{(3,2)} - \frac{2}{\sqrt{15}} \sigma_2^{-1} f_2 g^{(1,2)} - \frac{1}{\sqrt{3}} \sigma_0^{-1} f_0 g^{(1,0)}, \quad (2.23)$$

As seen from the above equations (2.21) and (2.23), the number of the couplings in the particle-dimer picture is larger than in the three-particle picture. Namely, one could argue that only two couplings in each set $h_J^{(I,I')}$ and $g^{(J,I)}$ are independent, and others can be chosen freely. Note that establishing the number of the independent couplings is a subtle dynamical issue and is discussed in detail in Ref. [59]. Here, we merely state that in the S-wave $\pi\pi$ scattering no shallow dimers exist that justifies a naive counting presented above. To fix the freedom, we choose $h_1^{(2,0)} = h_1^{(2,2)} = h_2^{(2,2)} = 0$ and $g^{(1,2)} = 3g^{(3,2)}$, $g^{(2,2)} = \sqrt{5}g^{(3,2)}$ (The latter two conditions ensures that, at tree level, the operators $T_{20}\pi_+$ and $T_{21}\pi_0$ are absent in the Lagrangian $\tilde{\mathcal{L}}_K$, which describes the weak decay of a kaon into the particle-dimer pair.).

An important question is, however, whether these redundant couplings, which are absent in the tree-level matching, re-emerge in the loops. We shall address this question in the following section.

2.5 Reduction of the redundant couplings

Following Eq. (2.19), one can trivially define a linear combination of the operators $\mathcal{O}_{J_3}^{(1,0)}$ and $\mathcal{O}_{J_3}^{(1,2)}$, which vanishes under the replacement (2.17). One need not display an explicit form of this linear combination here which, together with $\mathcal{O}_{J_3}^{(2,2)}$, forms a set of the *irrelevant* operators $\hat{\mathcal{O}}_{J_3}^{(a)}$, $a = 1, 2$. The contribution of the irrelevant operators to the physical matrix elements at tree-level vanishes. An orthogonal linear combination of $\mathcal{O}_{J_3}^{(1,0)}$ and $\mathcal{O}_{J_3}^{(1,2)}$ and $\mathcal{O}_{J_3}^{(3,2)}$ form a set of *relevant* operators $\mathcal{O}_{J_3}^{(a)}$, $a = 1, 2$. The question which will be addressed below, can be stated as follows: do the irrelevant operators contribute to the physical observables beyond the tree level? We shall demonstrate that this is not the case, and the irrelevant operators can be safely dropped from the beginning.

Let us start from the decay of a kaon into three pions, and consider the following vertex function

$$\hat{G}_{i_1 i_2 i_3}^{(a)}(x_1, x_2, x_3) = \langle 0 | T \left[O_{3\pi}^{i_1 i_2 i_3}(x_1, x_2, x_3) \left(\hat{\mathcal{O}}_1^{(a)} \right)^\dagger(0) \right] | 0 \rangle, \quad (2.24)$$

where $O_{3\pi}$ denotes a three-pion operator:

$$O_{3\pi}^{i_1 i_2 i_3}(x_1, x_2, x_3) = \pi_{i_1}(x_1) \pi_{i_2}(x_2) \pi_{i_3}(x_3). \quad (2.25)$$

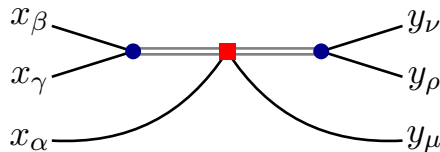


Figure 3. The tree-level contribution to the matrix element of the three-pion scattering. Black solid lines and gray double lines denote the particle propagator and the tree-level dimer propagator, respectively. The blue dots and the red rectangle correspond to the particle-dimer conversion vertex and the particle-dimer interaction vertex, respectively. The labels $(\alpha\beta\gamma)$ and $(\mu\nu\rho)$ denote the permutations of (123) .

At tree level, this vertex, shown in Fig. 2, vanishes, because of the Bose-symmetry of three pions in the final state. Now, note that the same vertex appears in any loop diagram that describes the kaon decay. It is straightforward to check that these loop diagrams vanish as well, since the tree-level vertex does not depend on the momenta of the final pions – in other words, it does not distinguish between the real and virtual pions. As a result, the contribution of the irrelevant operators to the pion decay amplitude vanishes to all orders in perturbation theory.

A similar argument applies for the three-pion scattering. The tree-level contribution to the quantity

$$\begin{aligned}
 & V_{i_1 i_2 i_3; j_1 j_2 j_3}^{(a,b)}(x_1, x_2, x_3; y_1, y_2, y_3) \\
 &= \langle 0 | T \left[O_{3\pi}^{i_1 i_2 i_3}(x_1, x_2, x_3) O_{3\pi}^{j_1 j_2 j_3}(y_1, y_2, y_3)^\dagger \sum_{J_3} \left(\mathcal{O}_{J_3}^{(a)}(0) \right)^\dagger \left(\hat{\mathcal{O}}_{J_3}^{(b)}(0) \right) \right] | 0 \rangle \quad (2.26)
 \end{aligned}$$

is shown in Fig. 3. Here, for simplicity, we assume that only one irrelevant operator appears, but the discussion in case of two irrelevant operators follows exactly the same path. The tree-level contribution, where each dimer line is equipped by two particle lines prior to escaping, obviously vanishes. The question, whether the irrelevant operators contribute in the loops reduces to the question, whether all internal dimer lines end up in the two-pion vertex. There is only one diagram, shown in Fig. 4, where this is not the case. However, the tree-level dimer propagator $S_I^{(0)}(x) = -\sigma_I^{-1} \delta^4(x)$ is local in position space. Hence, a closed loop over the non-relativistic pion propagator emerges, which vanishes due to the pole structure of the latter. To summarize, the irrelevant operators contribute neither to the kaon decay amplitudes, nor to the three-pion scattering amplitudes to all orders and, hence, can be safely discarded from the beginning.

3 Faddeev equations and derivation of the LL factor

3.1 Faddeev equation for particle-dimer amplitude

We start with writing down the Faddeev equation for the particle-dimer amplitude.⁸ There are three isospin channels with $J = 1, 2, 3$ (In the decays of charged kaons, the channel

⁸The Faddeev equations in the particle-dimer picture (both the non-relativistic and relativistic cases) has been considered in detail in the following papers [4, 46, 59, 80–82].

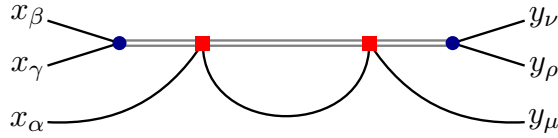


Figure 4. The particle-dimer loop diagram that could potentially contribute to the six-pion amplitude. Black solid lines and gray double lines denote a particle propagator and the tree-level dimer propagator, respectively. The blue dots and the red rectangle correspond to the particle-dimer conversion vertex and the particle-dimer interaction vertex, respectively.

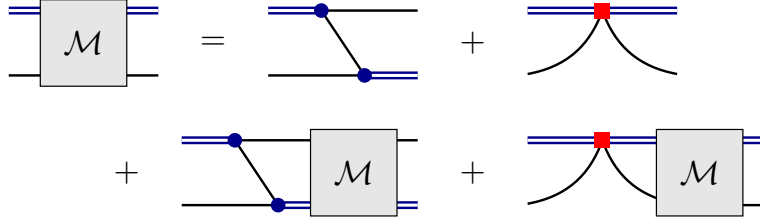


Figure 5. Faddeev equation for the particle-dimer scattering amplitude. The double blue line and the solid black line correspond to the full propagator of the dimer field the pion propagator, respectively. The blue circle denotes the vertex, converting the dimer to particles and the red box denotes the dimer-particle contact vertex. Isospin indices are implicit.

with $J = 0$ is excluded due to charge conservation.). It is important to note that, due to the symmetry properties of the three-pion wave function, the isospin channel $J = 2$ does not contribute to the kaon decay at the leading order. The particle-dimer amplitude $\mathcal{M}_{J;II'}(p, q; P)$ in an arbitrary reference frame defined by a unit vector v^μ obeys the equation

$$\mathcal{M}_{J;II'}(p, q; P) = Z_{J;II'}(p, q; P) + \sum_{I''} \int^{\Lambda_v} \frac{d^3 k_\perp}{(2\pi)^3 2w_v(k)} Z_{J;II''}(p, k; P) \tau_{I''}((P - k)^2) \mathcal{M}_{J;I''I'}(k, q; P). \quad (3.1)$$

Here, I and I' are the incoming and outgoing dimer isospin indices, p and q represent the on-shell four-momenta of outgoing/incoming particles, respectively, P is the total four-momentum of the three-pion system and $k_\perp^\mu = k^\mu - v^\mu(vk)$ denotes the perpendicular component of any vector k^μ in a frame defined by the unit vector v^μ , see also footnote 5. Furthermore, Λ_v denotes the ultraviolet cutoff which is defined by:

$$\int^{\Lambda_v} \frac{d^3 k_\perp}{(2\pi)^3} F(k) = \int \frac{d^4 k}{(2\pi)^3} \delta^4(k^2 - m^2) \theta(\Lambda^2 + k^2 - (vk)^2) F(k). \quad (3.2)$$

The Faddeev equation is diagrammatically illustrated in Fig. 5. Note that, in order to streamline the notations, we have changed the normalization of the amplitude, according to $\mathcal{M}_{J;II'} \rightarrow f_I^{-1} \mathcal{M}_{J;II'} f_{I'}^{-1}$. The quantity $Z_{J;II'}$ represents the driving term of the Faddeev equation while τ_I stands for the dimer propagator:

$$Z_{J;II'}(p, q; P) = \frac{c_{J;II'}}{2w_v(P - p - q)(w_v(P - p - q) + w_v(p) + w_v(q) - vP - i\varepsilon)} + \frac{H_{J;II'}(\Lambda)}{\Lambda^2},$$

$$\tau_I((P-k)^2) = f_I^2 S_I((P-k)^2). \quad (3.3)$$

The explicit expression for the quantity τ_I , which is directly related to the dimer propagator defined in Eq. (2.12), can be read off from Eq. (2.14). Furthermore, $c_{J;II'}$ are expressed through the Clebsh-Gordan coefficients and emerge after the projection onto the states with total isospin J :

$$c_{1;00} = \frac{1}{3}, \quad c_{1;02} = c_{1;20} = \frac{\sqrt{5}}{3}, \quad c_{1;22} = \frac{1}{6}, \quad c_{2;22} = -\frac{1}{2}, \quad c_{3;22} = 1. \quad (3.4)$$

Finally

$$H_{J;II'}(\Lambda) = \Lambda^2 f_I^{-1} h_J^{(I,I')} f_{I'}^{-1}. \quad (3.5)$$

According to the choice $h_1^{(2,0)} = h_1^{(2,2)} = h_2^{(2,2)} = 0$, only the couplings $H_{1;00}$ and $H_{3;22}$ are non-zero. Furthermore, as shown in Refs. [80, 81], if one restricts oneself only to the first term in $Z_{J;II'}$ and sets all $H_{J;II'}(\Lambda)$ to zero, the solution of the Faddeev equation is cutoff-dependent and shows oscillatory dependence on Λ . This cutoff-dependence is eliminated by adding the contribution from $H_{J;II'}(\Lambda)$. The Λ -dependence of these couplings is such that it exactly cancels the oscillatory behavior coming from the first term. For our case, two remarks are in order. First, as shown in Ref. [81], since the coefficient in the isospin-two channel, $c_{2;22} = -\frac{1}{2}$, has a negative sign, the amplitude even without the inclusion of $H_{2;22}(\Lambda)$ is cutoff-independent for all momenta $p \ll \Lambda$. Hence, one does not need to introduce the particle-dimer contact term in the $J = 2$ channel altogether. Second there are no physical dimers and hence there is only one independent three-pion amplitude in the $J = 1$ channel. Consequently, in this channel, it is sufficient to match the coupling $H_{1;00}$ only. To summarize, as expected from the beginning, all observable three-pion amplitudes can be made cutoff-independent by matching only two couplings $H_{1;00}$ and $H_{3;22}$, albeit the original particle-dimer Lagrangian contained four independent couplings. This statement does not hold, in general, for the (unobservable) particle-dimer amplitudes (We remind the reader that there are no shallow bound states in our case.).

For matching of $H_{J;II'}(\Lambda)$, we need the three-particle threshold amplitude and, equivalently, the particle-dimer threshold amplitude, which is obtained by setting $\mathbf{p}, \mathbf{q} = 0$ in the CM frame. This amplitude is singular at $E = 3M_\pi$. To get the regular part of this amplitude, we start with evaluating the amplitude slightly below threshold, assuming that $E = 3M_\pi - \varepsilon$, and consider the limit $\varepsilon \rightarrow 0$ at the end. Adding loops makes the singularity at $\varepsilon = 0$ weaker, and evaluating the diagrams up to two loops suffices for finding all singularities. Next, the singularities in ε are isolated and subtracted from the threshold amplitude, in order to obtain the regular part. This process is discussed in detail in Ref. [31] in a purely non-relativistic setting. The singularities in our case are the same and can be easily read off from Ref. [31]:

$$\begin{aligned} \mathcal{S}_{J;II'}(\varepsilon) &= \frac{1}{2M_\pi \varepsilon} c_{J;II'} - \frac{1}{2\sqrt{M_\pi \varepsilon}} \sum_{I''} (c_{J;II''} a_{I''} c_{J;I''I'}) \\ &\quad + \frac{\sqrt{3}}{2\pi} \log \frac{\varepsilon}{M_\pi} \sum_{I''} (c_{J;II''} a_{I''}^2 c_{J;I''I'}) \end{aligned}$$

$$-\frac{2}{3} \log \frac{\varepsilon}{M_\pi} \sum_{I'', I'''} (c_{J; I''} a_{I''} c_{J; I'' I'''} a_{I'''} c_{J; I'' I'''}). \quad (3.6)$$

In an arbitrary frame, the quantity ε should be defined as $\varepsilon = \sqrt{P^2} - 3M_\pi$, whereas \mathbf{p}, \mathbf{q} are replaced by p_\perp^μ, q_\perp^μ . By subtracting $\mathcal{S}_{J; I I'}$ from the threshold amplitude $\mathcal{M}_{J; I I'}$ and taking the limit $\varepsilon \rightarrow 0$, we get the regular particle-dimer threshold amplitude.

The infinite-volume three-particle amplitude⁹ is related to the particle-dimer amplitude in the following way:

$$T_{J; I I'}(\{p\}, \{q\}; P) = \sum_{\alpha, \beta=1}^3 \left[(2\pi)^3 \delta^3(p_{\alpha\perp} - q_{\beta\perp}) \delta_{I I'} 2w_v(p_\alpha) \tau_I((P - p_\alpha)^2) \right. \\ \left. + \tau_I((P - p_\alpha)^2) \mathcal{M}_{J; I I'}(p_\alpha, q_\beta; P) \tau_{I'}((P - q_\beta)^2) \right]. \quad (3.7)$$

Here, $\{p\}$ represents the set of all four-particle momenta p_α with $\alpha = 1, 2, 3$. The regular part of the three-particle amplitude can be related to the regular part of the particle-dimer amplitude in an obvious manner.

In a finite volume, the counterpart of the Faddeev equation can be written down as follows

$$\mathcal{M}_{J; I I'}^L(p, q; P) = Z_{J; I I'}(p, q; P) \\ + \sum_{I''} \frac{1}{L^3} \sum_{\mathbf{k}}^{\Lambda_v} \frac{1}{2w(\mathbf{k})} Z_{J; I I'}(p, k; P) \tau_{I''}^L(P - k) \mathcal{M}_{J; I'' I'}^L(k, q; P), \quad (3.8)$$

where L is the spatial extent of the box and finite-volume quantities are represented by the superscript L . The summation is over the discrete values of momentum $\mathbf{k} = 2\pi\mathbf{n}/L$, $\mathbf{n} \in \mathbb{Z}^3$. The finite volume propagator is given by

$$\tau_I^L(P) = \frac{16\pi\sqrt{s}}{16\pi\sqrt{s}[-\sigma_I f_I^{-2} - \frac{1}{2}J(s)] - \frac{2}{\sqrt{\pi}L\gamma} Z_{00}^{\mathbf{d}}(1; q_0^2)}, \quad (3.9)$$

where $s = P^2$ and the real part of the Chew-Mandelstam function, $J(s)$, is defined in Eq. (2.13). Furthermore, the Lüscher zeta-function $Z_{00}^{\mathbf{d}}(1; q_0^2)$ is defined as

$$Z_{00}^{\mathbf{d}}(1; q_0^2) = \frac{1}{\sqrt{4\pi}} \sum_{\mathbf{r}^2 \in P_d} \frac{1}{\mathbf{r}^2 - q_0^2}, \quad (3.10)$$

with $\gamma = \frac{P_0}{\sqrt{s}}$, $\mathbf{d} = \frac{L}{2\pi} \mathbf{P}$, $q_0^2 = \frac{L^2}{4\pi^2} \left(\frac{s}{4} - m^2 \right)$ and

$$P_d = \left\{ \mathbf{r} = \mathbb{R}^3 | r_{\parallel} = \gamma^{-1} \left(n_{\parallel} - \frac{1}{2} |\mathbf{d}| \right), \mathbf{r}_{\perp} = \mathbf{n}_{\perp}, \mathbf{n} \in \mathbb{Z}^3 \right\}.$$

The quantization condition, which now explicitly includes different isospin channels, is

⁹We would like to stress here that this is not a physical amplitude. The physical states with a given full isospin J can be built up from a pion and a dimer with a isospin I in different ways. In the quantity $T_{J; I I'}$, the full isospin J , as well as I, I' are fixed.

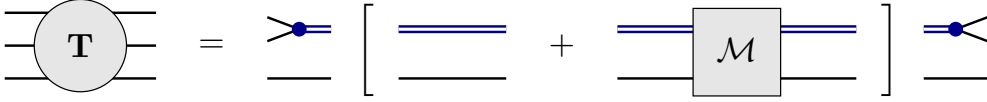


Figure 6. The three-particle amplitude in terms of the particle-dimer scattering amplitude. The sum over spectator momenta and the isospin indices are implicit.

given by

$$\det(A) = 0, \quad A_{J;II'}(p, q; P) = 2w(\mathbf{k})L^3\delta_{\mathbf{p}\mathbf{q}}\delta_{II'}[\tau_I^L(P-k)]^{-1} - Z_{J;II'}(p, q; P). \quad (3.11)$$

The finite-volume spectrum E_n of the three-particle system is determined by the discrete solutions of the quantization condition. The particle-dimer amplitude is factorized near the pole of the quantization condition as follows,

$$\mathcal{M}_{J;II'}^L(p, q; P)\Big|_{E \rightarrow E_n} = \frac{\phi_{J;I}^{(n)}(p)\phi_{J;I'}^{(n)}(q)}{P_{n,\parallel} - P_{\parallel} - i\varepsilon} + \text{regular},$$

where $\phi_{J;I}^{(n)}(p)$ is the finite-volume particle-dimer wave function and it obeys the homogeneous equation:

$$\phi_{J;I}^{(n)}(p) = \sum_{I'} \frac{1}{L^3} \sum_{\mathbf{k}}^{\Lambda_v} \frac{1}{2w(\mathbf{k})} Z_{J;II'}(p, k; P) \tau_{I'}^L(P-k) \phi_{J;I'}^{(n)}(k). \quad (3.12)$$

Note that $Z_{J;II'}(p, k; P)$ and $\tau_{I'}^L(P-k)$ are energy-dependent quantities and hence the wave function is not normalized to unity but rather obeys the following normalization condition

$$\begin{aligned} \sum_{II'} \frac{1}{L^6} \sum_{\mathbf{p}, \mathbf{k}}^{\Lambda_v} \phi_{J;I}^{(n)}(p) \frac{\tau_I^L(P-p)}{2w(\mathbf{p})} \frac{dZ_{J;II'}(p, k; P)}{dP_{n,\parallel}} \frac{\tau_{I'}^L(P-k)}{2w(\mathbf{k})} \phi_{J;I'}^{(n)}(k) \\ + \sum_I \frac{1}{L^3} \sum_{\mathbf{p}}^{\Lambda_v} \phi_{J;I}^{(n)}(p) \frac{1}{2w(\mathbf{p})} \frac{d\tau_I^L(P-p)}{dP_{n,\parallel}} \phi_{J;I}^{(n)}(p) = 1, \end{aligned} \quad (3.13)$$

where one substitutes $P_{\parallel} = P_{n,\parallel}$ after differentiation.

3.2 Matching of the three-pion coupling

Below, we shall perform the matching of the particle-dimer couplings to the three-pion threshold amplitude. These amplitudes will be evaluated at tree level in perturbation theory.¹⁰ We start from calculating the physical three-particle amplitudes in the particle basis.¹¹ In order to express these in terms of particle-dimer amplitudes, one has to equip

¹⁰Note that, within the RFT approach, this matching has been carried out at one loop recently [63]. Here, we restrict ourselves to the tree-level calculations. Anyway, it will be demonstrated below that, in the LL factor we are after, there is barely any dependence on the exact value of the threshold tree-body amplitude.

¹¹There are only two independent six-pion couplings at lowest order. This means that one can use any two linearly independent physical amplitudes to perform the matching. We use $3\pi^+ \rightarrow 3\pi^+$ and $3\pi^0 \rightarrow 3\pi^0$ amplitudes for this purpose here.

the latter by the full dimer propagators for the outgoing legs and the vertex functions that describe the transition of a dimer into a two-pion pair, see Eq. (3.7). The (connected part of the) threshold amplitude for the scattering of three charged pions is straightforward to obtain, since it contains only the isospin $J = 3$ contribution:

$$T^{\text{conn}}(3\pi^+ \rightarrow 3\pi^+) = 9\mathcal{M}_{3;22}(\varepsilon)\tau_2(\varepsilon)^2. \quad (3.14)$$

Here, the factor 9 comes after summation over all permutations of the external lines. Similarly, the connected part of the amplitude with three neutral pions is given by

$$\begin{aligned} T^{\text{conn}}(3\pi^0 \rightarrow 3\pi^0) &= 3\mathcal{M}_{1;00}(\varepsilon)\tau_0^2(\varepsilon) + \frac{12}{\sqrt{5}}\mathcal{M}_{1;02}(\varepsilon)\tau_0(\varepsilon)\tau_2(\varepsilon) \\ &+ \frac{12}{5}\mathcal{M}_{1;22}(\varepsilon)\tau_2(\varepsilon)^2 + \frac{18}{5}\mathcal{M}_{3;22}(\varepsilon)\tau_2(\varepsilon)^2. \end{aligned} \quad (3.15)$$

The amplitudes entering the above equations are defined as

$$\begin{aligned} \mathcal{M}_{J;II'}(\varepsilon) &= \mathcal{M}_{J;II'}(\varepsilon)(\bar{p}, \bar{q}; \bar{P}), \quad \tau_I(\varepsilon) = \tau_I((\bar{P} - \bar{p})^2), \\ \bar{p} = \bar{q} &= (M_\pi, \mathbf{0}), \quad \bar{P} = (3M_\pi - \varepsilon, \mathbf{0}). \end{aligned} \quad (3.16)$$

Furthermore, according to Eqs. (3.6) and (2.14), the expansion of $\mathcal{M}_{J;II'}(\varepsilon)$ and $\tau_I(\varepsilon)$ in ε takes the following form:

$$\begin{aligned} \mathcal{M}_{J;II'}(\varepsilon) &= \frac{c_{J;II'}}{2M_\pi\varepsilon} + \frac{d_{J;II'}}{2\sqrt{M_\pi\varepsilon}} + e_{J;II'} \log \frac{\varepsilon}{M_\pi} + \bar{\mathcal{M}}_{J;II'} + \mathcal{O}(\sqrt{\varepsilon}), \\ \tau_I(\varepsilon) &= -32\pi M_\pi a_I \left(1 + a_I \sqrt{M_\pi\varepsilon} + a_I^2 M_\pi\varepsilon - \frac{2a_I\varepsilon}{\pi} \right), \end{aligned} \quad (3.17)$$

where $d_{J;II'}$ and $e_{J;II'}$ are coefficients that are proportional to the powers of the two-body scattering length. Therefore, applying chiral power counting, from Eq. (3.6) it directly follows that

$$c_{J;II'} = \mathcal{O}(1), \quad d_{J;II'} = \mathcal{O}(M_\pi^2), \quad e_{J;II'} = \mathcal{O}(M_\pi^4). \quad (3.18)$$

Taking into account the fact that the tree-level amplitude in ChPT, which will be matched to the six-point amplitudes given in Eqs. (3.14) and (3.15), is of order M_π^2 (see appendix B), it follows that, at the accuracy we are working, the regular part of these amplitudes (i.e., the piece that is obtained from the amplitudes after dropping all divergent pieces in ε and performing the limit $\varepsilon \rightarrow 0$) is given by

$$\begin{aligned} T_{\text{reg}}^{\text{conn}}(3\pi^+ \rightarrow 3\pi^+) &= 9\bar{\mathcal{M}}_{3;22}\bar{\tau}_2^2, \\ T_{\text{reg}}^{\text{conn}}(3\pi^0 \rightarrow 3\pi^0) &= 3\bar{\mathcal{M}}_{1;00}\bar{\tau}_0^2 + \frac{12}{\sqrt{5}}\bar{\mathcal{M}}_{1;02}\bar{\tau}_0\bar{\tau}_2 + \frac{12}{5}\bar{\mathcal{M}}_{1;22}\bar{\tau}_2^2 + \frac{18}{5}\bar{\mathcal{M}}_{3;22}\bar{\tau}_2^2, \end{aligned} \quad (3.19)$$

where $\bar{\tau}_I = 32\pi M_\pi a_I$, and $\bar{\mathcal{M}}_{J;II'}$ denotes the regular part of the particle-dimer scattering amplitude.

These amplitudes can be matched to the ones obtained from ChPT, see the appendix B. The result there is given by

$$T_+^\chi = \frac{18M_\pi^2}{F_\pi^4}, \quad T_0^\chi = -\frac{9M_\pi^2}{8F_\pi^4}. \quad (3.20)$$

The three-pion couplings $H_{1;00}(\Lambda)$ and $H_{3;22}(\Lambda)$ can be determined by numerically solving the Faddeev equation, extracting the threshold particle-dimer amplitudes $\bar{\mathcal{M}}_{J;I'}$ from these solutions after subtracting the divergent pieces, and then equating the result given in Eq. (3.19), to $T_{+,0}^\chi$.

3.3 Derivation of the LL factor

The LL factor connects the decay amplitudes between the infinite volume and a finite volume. Therefore, in order to obtain the LL factor, we need to calculate the amplitude of $K \rightarrow 3\pi$ twice, separately in the infinite volume and in a finite volume.

In the infinite volume, we calculate the decay amplitude in two steps. First, K decays into a dimer and a spectator pion. Then, the dimer further decays into two pions. The final state at threshold can have the total isospin $J = 1, 3$. Assuming, for convenience that $J_3 = 1$, we get

$$\langle \pi^{i_1}(p_1)\pi^{i_2}(p_2)\pi^{i_3}(p_3)|K^+ \rangle = \sum_{\alpha} \sum_I \mathcal{A}(K^+ \rightarrow T_{I,(1-i_\alpha)}\pi^{i_\alpha}(p_\alpha)) \langle 1, i_\beta; 1, i_\gamma | I, (1-i_\alpha) \rangle, \quad (3.21)$$

with $\alpha\beta\gamma = (123), (231), (312)$. The amplitude for K^+ decaying into a dimer and a pion can be expressed as

$$\mathcal{A}(K^+ \rightarrow T_{I,(1-i_\alpha)}\pi^{i_\alpha}) = \sum_J \langle I, (1-i_\alpha); 1, i_\alpha | J, 1 \rangle \left(g^{(J,I)}\tau_I + \sum_{I'} \tau_I \Phi_{J;I'I'} g^{(J,I')} \right). \quad (3.22)$$

where the amplitude Φ in the CM frame is defined as

$$\Phi_{J;I'I'}(\mathbf{p}) = \int^\Lambda \frac{d^3\mathbf{q}}{(2\pi)^3 2w(\mathbf{q})} \mathcal{M}_{J;I'I'}(\mathbf{p}, \mathbf{q}; E) \tau_{I'}(\mathbf{q}; E), \quad (3.23)$$

where $\tau_{I'}(\mathbf{q}; E)$ stands for $\tau_{I'}((P-q)^2)$ with $P^\mu = (E, \mathbf{0})$ and $q^\mu = (\sqrt{M_\pi^2 + \mathbf{q}^2}, \mathbf{q})$. From the Faddeev equation for the particle-dimer scattering amplitude (3.1), the equation for the amplitude Φ can be derived:

$$\Phi_{J;I'I'}(\mathbf{p}) = \sum_{I''} \int^\Lambda \frac{d^3\mathbf{q}}{(2\pi)^3 2w(\mathbf{q})} Z_{J;I'I''}(\mathbf{p}, \mathbf{q}; E) \tau_{I''}(\mathbf{q}; E) \left(\delta_{I''I'} + \Phi_{J;I''I'}(\mathbf{q}) \right), \quad (3.24)$$

Using Eqs. (3.21), (3.22) and performing the projection onto the S-wave, for the charged (“c”) and the neutral (“n”) channels we obtain

$$\begin{pmatrix} \langle \pi^+(p_1)\pi^+(p_2)\pi^-(p_3)|K^+ \rangle \\ \langle \pi^0(p_1)\pi^0(p_2)\pi^+(p_3)|K^+ \rangle \end{pmatrix} = \begin{pmatrix} X_{c0} & X_{c2} \\ X_{n0} & X_{n2} \end{pmatrix} \begin{pmatrix} g^{(1,0)} \\ g^{(3,2)} \end{pmatrix}, \quad (3.25)$$

where we took into account the constraints $g^{(1,2)} = 3g^{(3,2)}$ and $g^{(2,2)} = \sqrt{5}g^{(3,2)}$ already. The entries of the matrix X are:

$$X_{c0} = \frac{\tau_0(p_1)}{\sqrt{3}} \left[1 + \Phi_{1;00}(p_1) \right] + \frac{\tau_2(p_1)}{2\sqrt{15}} \Phi_{1;20}(p_1) + (p_1 \rightarrow p_2) + \frac{3\tau_2(p_3)}{\sqrt{15}} \Phi_{1;20}(p_3),$$

$$\begin{aligned}
X_{c2} &= \sqrt{3}\tau_0(p_1)\Phi_{1;02}(p_1) + \sqrt{\frac{3}{20}}\tau_2(p_1)\left[\frac{5}{3} + \Phi_{1;22}(p_1) + \frac{2}{3}\Phi_{3;22}(p_1)\right] + (p_1 \rightarrow p_2) \\
&\quad + \sqrt{15}\tau_2(p_3)\left[\frac{2}{3} + \frac{3}{5}\Phi_{1;22}(p_3) + \frac{1}{15}\Phi_{3;22}(p_3)\right], \\
X_{n0} &= -\frac{3\tau_2(p_1)}{2\sqrt{15}}\Phi_{1;20}(p_1) + (p_1 \rightarrow p_2) - \frac{\tau_0(p_3)}{\sqrt{3}}\left[1 + \Phi_{1;00}(p_3)\right] + \frac{\tau_2(p_3)}{\sqrt{15}}\Phi_{1;20}(p_3), \\
X_{n2} &= -\sqrt{\frac{27}{20}}\tau_2(p_1)\left[\frac{5}{9} + \Phi_{1;22}(p_1) - \frac{4}{9}\Phi_{3;22}(p_1)\right] + (p_1 \rightarrow p_2) \\
&\quad - \sqrt{3}\tau_0(p_3)\Phi_{1;02}(p_3) + \sqrt{\frac{3}{5}}\tau_2(p_3)\left[\frac{5}{3} + \Phi_{1;22}(p_3) + \frac{2}{3}\Phi_{3;22}(p_3)\right]. \tag{3.26}
\end{aligned}$$

Note also that we denote $p_i = |\mathbf{p}_i|$.

In a finite volume, our aim is to compute the matrix element $\langle \Gamma n, J | K^+ \rangle$. Here, $\langle \Gamma n, J |$ refers to the state on the lattice, carrying total isospin J , total momentum \mathbf{d} (in units of $2\pi/L$), and residing in the irrep Γ , corresponding to the n -th energy level¹² This matrix element can be calculated using the wave function in a finite volume [59]:

$$\langle \Gamma n, J | K^+ \rangle = \frac{1}{L^{3/2}} \left(\frac{M_K}{\sqrt{M_K^2 + \left(\frac{2\pi\mathbf{d}}{L}\right)^2}} \right)^{1/2} \sum_I \frac{1}{L^3} \sum_{\mathbf{k}}^{\Lambda_v} \frac{1}{2w(\mathbf{k})} \phi_{J;I}^{(n)}(\mathbf{k}) \tau_I^L(\mathbf{k}; E) g^{(J,I)}. \tag{3.27}$$

Here, $\phi_{J;I}^{(n)}(\mathbf{k})$ represents the Bethe-Salpeter wave function describing the state $|\Gamma n, J\rangle$, Furthermore, \mathbf{k} is the momentum of the spectator, and I is the isospin of the dimer, Λ_v means that cutoff on \mathbf{k} is imposed in a moving system with velocity v [46]. To calculate the wave function $\phi_{JI}^{(n)}(\mathbf{k})$, we first project the Faddeev equation onto irreps Γ , i.e.,

$$\begin{aligned}
\mathcal{M}_{J;II'}^{(\Gamma)}(r, r') &= Z_{J;II'}^{(\Gamma)}(r, r') \\
&\quad + \sum_{I''} \frac{1}{GL^3} \sum_s^{\Lambda_v} \left(\frac{\vartheta_s}{2w_s} \right) Z_{J;II'}^{(\Gamma)}(r, s) \tau_{I''}^L(s) \mathcal{M}_{J;I''I'}^{(\Gamma)}(s, r'). \tag{3.28}
\end{aligned}$$

In the projected equation, the momenta of the spectator particles are replaced by shell indices r, r' and s . We use ϑ_s to represent the multiplicity of the shell s , while G denotes the number of elements in the discrete symmetry group that leaves the total three-momentum of the system invariant. The projection of τ and Z is performed, according to the method of Ref. [83]

$$\tau^L(s) = \tau^L(\mathbf{k}_0(s)), \quad Z_{J;II'}^{(\Gamma)}(r, s) = \sum_{g \in \mathcal{G}} \left(T^{(\Gamma)}(g) \right)^\dagger Z_{J;II'}(g\mathbf{p}_0(r), \mathbf{k}_0(s)). \tag{3.29}$$

¹²Here, the size of the lattice is L . This parameter should be adjusted so that the energy E_n exactly equals to M_K . The label n is used for different eigenvalues. In order to avoid the clutter of indices, we have opted for lumping the irrep index Γ , as well as the total momentum \mathbf{d} together with the level index n and hope that this will not lead to a confusion.

Here $T^{(\Gamma)}(g)$ is the representation matrix and the momenta $\mathbf{p}_0(r)$ and $\mathbf{k}_0(s)$ are the reference vectors of the r -shell and the s -shell, respectively. Based on this, it is not difficult to deduce that the wave function is a solution to the homogeneous equation,

$$\phi_{J;I}^{(n)}(r) = \sum_{I'} \frac{1}{GL^3} \sum_s \left(\frac{\vartheta_s}{2w_s} \right) Z_{J;I'I}^{(\Gamma)}(r, s) \tau_{I'}^L(s) \phi_{J;I'}^{(n)}(s). \quad (3.30)$$

The solutions of the equation should be normalized, according to [59]

$$\begin{aligned} & \sum_{r,s} \sum_{I,I'} \frac{\vartheta_r}{2w_r L^3} \frac{\vartheta_s}{2w_s L^3} \phi_{JI}^{(n)}(r) \tau_I^L(r) \mathbb{P}_{J;I'I'}(r, s) \tau_{I'}^L(s) \phi_{J'I'}^{(n)}(s) \\ & - \sum_r \sum_I \frac{\vartheta_r}{2w_r L^3} \phi_{JI}^{(n)}(r) \tau_I^L(r) \mathbb{Q}_I(r) \tau_I^L(r) \phi_{JI}^{(n)}(r) = 1. \end{aligned} \quad (3.31)$$

Here

$$\mathbb{P}_{J;I'I'}(r, s) = \frac{\partial}{\partial P_{\parallel}} Z_{J;I'I}^{\Gamma}(r, s), \quad \mathbb{Q}_I(r) = \frac{\partial}{\partial P_{\parallel}} \left(\tau_I^L(r) \right)^{-1}. \quad (3.32)$$

The time-like component P_{\parallel} is obtained from total four-momentum P^{μ} :

$$P_{\parallel} = v \cdot P = \sqrt{P^2}. \quad (3.33)$$

Similar to the infinite-volume case, we can define the finite-volume amplitude Φ :

$$\Phi_{J;I}^{(n)} = \frac{1}{L^3} \sum_{\mathbf{k}}^{\Lambda_v} \frac{1}{2w(\mathbf{k})} \phi_{J;I}^{(n)}(\mathbf{k}) \tau_I^L(\mathbf{k}; E) = \frac{1}{L^3} \sum_r^{\Lambda_v} \left(\frac{\vartheta_r}{2w_r} \right) \phi_{J;I}^{(n)}(r) \tau_I^L(r). \quad (3.34)$$

Therefore, we have

$$\langle \Gamma n, J | K^+ \rangle = \frac{1}{L^{3/2}} \left(\frac{M_K}{\sqrt{M_K^2 + \left(\frac{2\pi \mathbf{d}}{L} \right)^2}} \right)^{1/2} \sum_I \Phi_{J;I}^{(n)} g^{(J,I)}. \quad (3.35)$$

Finally, one obtains:

$$\begin{pmatrix} L^{3/2} \langle \Gamma n, 1 | K^+ \rangle \\ L^{3/2} \langle \Gamma n, 3 | K^+ \rangle \end{pmatrix} = \begin{pmatrix} A_{10} & A_{12} \\ A_{30} & A_{32} \end{pmatrix} \begin{pmatrix} g^{(1,0)} \\ g^{(3,2)} \end{pmatrix}. \quad (3.36)$$

Here, matrix element A_{JI} is given by

$$A_{JI} = \left(\frac{M_K}{\sqrt{M_K^2 + \left(\frac{2\pi \mathbf{d}}{L} \right)^2}} \right)^{1/2} a_{JI} \Phi_{J;I}^{(n)}, \quad (3.37)$$

and the coefficients a_{JI} are

$$a_{10} = 1, \quad a_{12} = 3, \quad a_{30} = 0, \quad a_{32} = 1. \quad (3.38)$$

The decay amplitudes both in a finite and in the infinite volume are expressed through the same couplings $g^{(1,0)}$ and $g^{(3,2)}$, see Eqs. (3.25) and (3.36). Excluding these couplings, we obtain the LL factor for $K \rightarrow 3\pi$ which, in this case, is a 2×2 matrix:

$$\begin{pmatrix} \langle \pi^+ \pi^+ \pi^- | K^+ \rangle \\ \langle \pi^0 \pi^0 \pi^+ | K^+ \rangle \end{pmatrix} = \begin{pmatrix} \mathbb{L}_{c1} & \mathbb{L}_{c3} \\ \mathbb{L}_{n1} & \mathbb{L}_{n3} \end{pmatrix} \begin{pmatrix} L^{3/2} \langle \Gamma n, 1 | K^+ \rangle \\ L^{3/2} \langle \Gamma n, 3 | K^+ \rangle \end{pmatrix}, \quad (3.39)$$

where

$$\begin{pmatrix} \mathbb{L}_{c1} & \mathbb{L}_{c3} \\ \mathbb{L}_{n1} & \mathbb{L}_{n3} \end{pmatrix} = \begin{pmatrix} X_{c0} & X_{c2} \\ X_{n0} & X_{n2} \end{pmatrix} \begin{pmatrix} A_{10} & A_{12} \\ A_{30} & A_{32} \end{pmatrix}^{-1}. \quad (3.40)$$

The explicit expression for the 3-particle LL factor, given by the above formulae, represents one of the main results of the present work.

4 Numerical calculation of LL factor

4.1 Solution of the Faddeev equation in the infinite volume

In order to solve Eq. (3.24) in the infinite volume, we need to first study the analytic properties of the kernel. For simplicity, we restrict ourselves to the CM system and use the notation $p = |\mathbf{p}|$, $q = |\mathbf{q}|$ and $z = \cos \theta$, where θ is the angle between \mathbf{p} and \mathbf{q} . It is straightforwardly seen that the singularity of $Z(\mathbf{p}, \mathbf{q}; E)$ is determined by the three-body on-shell condition¹³,

$$\sqrt{p^2 + q^2 + 2pqz + M_\pi^2} + \sqrt{p^2 + M_\pi^2} + \sqrt{q^2 + M_\pi^2} = E, \quad (4.1)$$

with $-1 \leq z \leq 1$. As known [84–87], one can avoid these (logarithmic) singularities by deforming the contour into the complex plane (see Fig. 7(a)). In our case, the contour can be chosen as follows,

$$q = \begin{cases} t - i\mu(1 - e^{-t/\sigma})(1 - e^{(t-B_{\max})/\sigma}), & (0 < t < B_{\max}) \\ t, & (B_{\max} < t < \Lambda) \end{cases} \quad (4.2)$$

where the parameters are

$$\delta = 0.5M_\pi, \quad \sigma = M_\pi, \quad \mu = 0.1M_\pi, \quad B_{\max} = p_t + \delta. \quad (4.3)$$

Here p_t is the magnitude of the momentum of the spectator, for which the two-body system is exactly at threshold. If $|\mathbf{p}| > p_t$, the two-body system moves below threshold. This gives

$$(E - w(\mathbf{p}))^2 - \mathbf{p}^2 \leq 4M_\pi^2, \quad (4.4)$$

and

$$p \geq \sqrt{\left(\frac{E^2 - 3M_\pi^2}{2E}\right)^2 - M_\pi^2} = p_t. \quad (4.5)$$

¹³In principle, the dimer propagator τ_L also has singularities, but they are irrelevant to our calculation.

The solution of the equation (3.24) proceeds step by step. First, after projecting onto the S-wave, one solves this equation with both the momenta p and q belonging to the contour C :

$$\Phi_{J;II'}(p) = \sum_{I''} \int_C \frac{q^2 dq}{2\pi^2 2w(q)} Z_{J;II''}(p, q; E) \tau_{I''}(q; E) (\delta_{I''I'} + \Phi_{J;I''I'}(q)). \quad (4.6)$$

The integrand is never singular on the integration contour C . This can be visualized in Fig. 7(a), where the shaded area is obtained as follows. The total energy $E = M_K$ is fixed. We first choose the momentum p on the contour and plot the curve for q , obtained by the solution of Eq. (4.1) for $-1 \leq z \leq 1$. Changing then p with a very small step along the contour, we arrive at a new curve. Repeating this procedure many times, we arrive at a shaded area that does not intersect with our integration curve. Hence, for p and q both on the curve, the kernel Z never becomes singular, and the integral equation can be straightforwardly transformed into a set of linear equations by discretizing the integration with the use of the fixed mesh points and weights. We are ultimately interested, however, in the amplitude $\Phi_{J;II'}(p)$ on the real axis, which can be obtained by analytically continuing $\Phi_{J;II'}(p)$, defined by the Eq. (4.6) to the real axis, whereas the argument q , over which the integration is performed, still stays on the the contour C . In doing so, it is important to check that one does not hit the singularities of the kernel Z during this analytic continuation. Below, we shall address this issue in detail.

Let us define the quantity

$$p_0 \equiv \sqrt{\left(\frac{E - M_\pi}{2}\right)^2 - M_\pi^2} \quad (4.7)$$

It turns out that there are three different regions of p [85, 88]:

1. When $p < p_0$, the singularities of $Z(p, q; E)$ lie just above and below the real axis,¹⁴ see Fig. 7(b). Our contour does not intersect with any of these branch cuts and the integration can be safely performed.
2. For $p_0 < p < p_t$, The branch cuts move into the complex plane and start to intersect with the chosen contour, see Fig. 7(c). In order to avoid the singularities, one has to deform the integration contour as well. The new contour, C^+ , consists of two parts:

Part 1: Starting from the origin, it follows the positive real axis until the beginning of the branch cut located at the first singularity of the kernel at $q = q_1$, where q_1 is given by

$$q_1 = \frac{p}{2} - \frac{\varepsilon(p)}{2} \left(1 - \frac{4M_\pi^2}{\varepsilon^2(p) - p^2}\right)^{1/2}, \quad \varepsilon(p) = E - w(p). \quad (4.8)$$

¹⁴Remember that the energy E has infinitesimal positive imaginary part.

After reaching q_1 , the contour dives to the second Riemann sheet and goes back to the origin along the real axis. The contribution of this part to the integral is given by

$$\begin{aligned}
& \Phi_{J;II'}^{(1)}(p) \\
&= \sum_{I''} \left(\int_{0+i\varepsilon}^{q_1+i\varepsilon} + \int_{q_1-i\varepsilon}^{0-i\varepsilon} \right) \frac{q^2 dq}{2\pi^2 2w(q)} Z_{J;II''}(p, q; E) \tau_{I''}(q; E) \left(\delta_{I''I'} + \Phi_{J;I''I'}(q) \right) \\
&= \sum_{I''} \int_0^{q_1} \frac{q^2 dq}{2\pi^2 2w(q)} \left[Z_{J;II''}(p, q; E) - Z_{J;II''}^{(II)}(p, q; E) \right] \tau_{I''}(q; E) \left(\delta_{I''I'} + \Phi_{J;I''I'}(q) \right).
\end{aligned} \tag{4.9}$$

The kernel $Z_{J,II'}$, projected on any partial wave, is expressed through a logarithmic function. Since the discontinuity is caused solely by this logarithm, we conclude that the kernel on the second Riemann sheet, $Z^{(II)}$ is obtained from Z by replacing the $\log z$ with $\log z + 2\pi i$. Furthermore, since $q_1 < p_0$, the function $\Phi(q)$ is known along the real axis and the integral is completely defined.

Part 2: The second part of the path starts from the origin of the second Riemann sheet, following path C to reach the intersection point q_2 with the branch cut. Returning through q_2 to the first Riemann sheet, it continues along path C to reach the integration endpoint Λ , that is

$$\begin{aligned}
\Phi_{J;II'}^{(2)}(p) &= \sum_{I''} \int_0^{q_2} \frac{q^2 dq}{2\pi^2 2w(q)} Z_{J;II''}^{(II)}(p, q; E) \tau_{I''}(q; E) \left(\delta_{I''I'} + \Phi_{J;I''I'}(q) \right) \\
&+ \sum_{I''} \int_{q_2}^{\Lambda} \frac{q^2 dq}{2\pi^2 2w(q)} Z_{J;II''}(p, q; E) \tau_{I''}(q; E) \left(\delta_{I''I'} + \Phi_{J;I''I'}(q) \right) \\
&= \sum_{I''} \int_C \frac{q^2 dq}{2\pi^2 2w(q)} \tilde{Z}_{J;II''}(p, q; E) \tau_{I''}(q; E) \left(\delta_{I''I'} + \Phi_{J;I''I'}(q) \right).
\end{aligned} \tag{4.10}$$

The quantity \tilde{Z} is defined in the following way:

$$\tilde{Z}_{J;II'}(p, q; E) = \begin{cases} Z_{J;II'}^{(II)}(p, q; E), & f(p, q; E) < 0 \\ Z_{J;II'}(p, q; E), & f(p, q; E) \geq 0 \end{cases}. \tag{4.11}$$

Here, $f(p, q; E)$ is defined by

$$f(p, q; E) = \left((\text{Re}q)^2 + (\text{Im}q)^2 \right)^2 + m^2 (d^2(p) - b^2(p)) \left(\frac{(\text{Re}q)^2}{d^2(p)} + \frac{(\text{Im}q)^2}{b^2(p)} \right), \tag{4.12}$$

with

$$b(p) = \frac{\varepsilon(p)}{p}, \quad d(p) = \frac{\varepsilon^2(p) - p^2}{2mp}. \tag{4.13}$$

Finally, in the region $p_0 < p < p_t$, the full amplitude is given by

$$\Phi_{J;II'}(p) = \Phi_{J;II'}^{(1)}(p) + \Phi_{J;II'}^{(2)}(p). \tag{4.14}$$

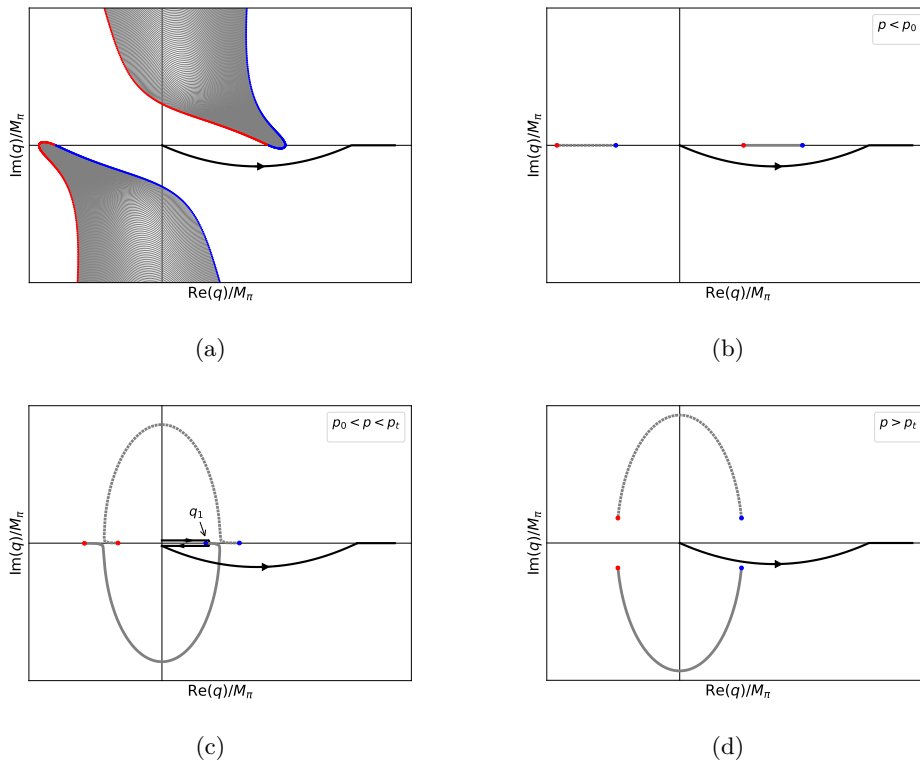


Figure 7. In panel (a), the contour and the domain of the singularity of the kernel Z is shown. It is clear that, when both momenta are located on the deformed contour, the kernel does not become singular. In the panels (b,c,d), the choice of the integration contour for the calculation of the amplitude Φ on the real axis is displayed for three different choices, $p < p_0$, $p_0 < p < p_t$, and $p > p_t$, respectively. In the second case, the path should be deformed from the original one, in order to avoid the singularities of the kernel (see the discussion in the text).

3. When $p > p_t$, the branch cuts of the function Z move into the complex plane and do not intersect with our contour C anymore,¹⁵ see Fig. 7(d). Therefore, it is again safe to integrate over the initial contour.

By using the techniques described above, we can calculate the amplitudes $\Phi_{1;00}$, $\Phi_{1;02}$, $\Phi_{1;20}$, $\Phi_{1;22}$ and $\Phi_{3;22}$ on the real axis. These solutions are displayed in Fig. 9. We choose the cutoff $\Lambda = 15M_\pi$ and matched the couplings $H_{1;00}$ and $H_{3;22}$ to the tree-level threshold amplitudes in ChPT as described above. Varying the cutoff, but keeping the threshold amplitude fixed, it can be shown that the three-body couplings exhibit singular behavior

¹⁵In principle, when $p > p_t$ but very close to p_t , the branch cut may still intersect with the contour. Strictly speaking, for any given $p > p_t$, one may choose the parameter μ small enough that there is no intersection. On the contrary, for any fixed finite μ , one may find an interval between p_t and $p_t + \varepsilon'$, when the branch cut and the contour intersect. The quantity ε' depends on μ and tends to zero at $\mu \rightarrow 0$. In practical terms, it means that one is not able to determine the solution for $p \in [p_t, p_t + \varepsilon']$ by using the method described here. The length of this interval can be however made arbitrary small with the choice of μ . This does not create problems in actual calculations, while ε' turns out to be extremely small.

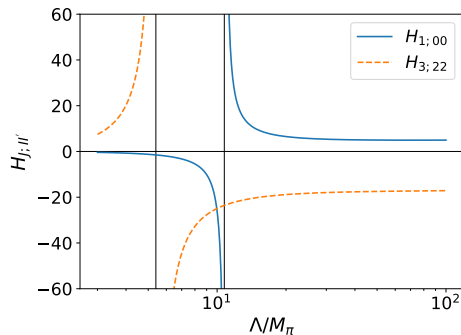


Figure 8. The running of the three-body couplings $H_{1;00}$ and $H_{3;22}$ with respect to the cutoff Λ .

that resembles the log-periodic running in the unitary limit, see Fig. 8. Note also that the LL factor should be cutoff-independent that will be explicitly demonstrated below.

Next, in order to estimate the dependence on the kinematical variables, we shall calculate the quantities X_{c0} , X_{c2} , X_{n0} and X_{n2} , defined by Eq. (3.26), which enter the expression of the LL factor. In the CM frame, the total energy is fixed to be the mass of the kaon, i.e., $E = M_K \simeq 3.54M_\pi$. These quantities depend on the momenta of outgoing pions that can be parameterized by two invariant variables $m_{12}^2 = (p_1 + p_2)^2$ and $m_{23}^2 = (p_2 + p_3)^2$. In Fig. 10, we display the Dalitz plots for the quantities X_{c0} , X_{c2} , X_{n0} , X_{n2} that emerge in a result of such calculations.

4.2 Finite-volume wave function

In order to calculate Φ in a finite volume, we first need to adjust the lattice size L so that one has the energy level with the energy exactly equal to the kaon mass. Solving the three-body quantization condition in the rest frame and in the different moving frames, we obtain the energy spectrum, see Fig. 11 and Fig. 12. For demonstration, we choose the moving frame with the total momentum $(0, 0, 1)$ (in units of $2\pi/L$). In the channels with the total isospin $J = 1$ and $J = 3$, respectively, the adjusted lattice size is given by

$$J = 1 : \quad L = 3.55M_\pi^{-1}; \quad (4.15)$$

$$J = 3 : \quad L = 4.09M_\pi^{-1}. \quad (4.16)$$

Once the lattice size is determined, we proceed to solve the Eq. (3.30) in order to obtain the (properly normalized) wave function in a finite volume. In its turn, this wave function will be substituted into Eq. (3.34) to find the amplitudes $\Phi_{J;I}^{(n)}$ that enter the expression of the LL factor, see Eq. (3.37).

4.3 The LL factor

Putting pieces together, in this section we present the results of the calculation of the LL factor, check its cutoff-dependence and the sensitivity to the input two-body scattering lengths and the three-particle amplitudes. To this end, we shall carry out calculations for three different values of the cutoff. Furthermore, the LL factor depends on the momenta

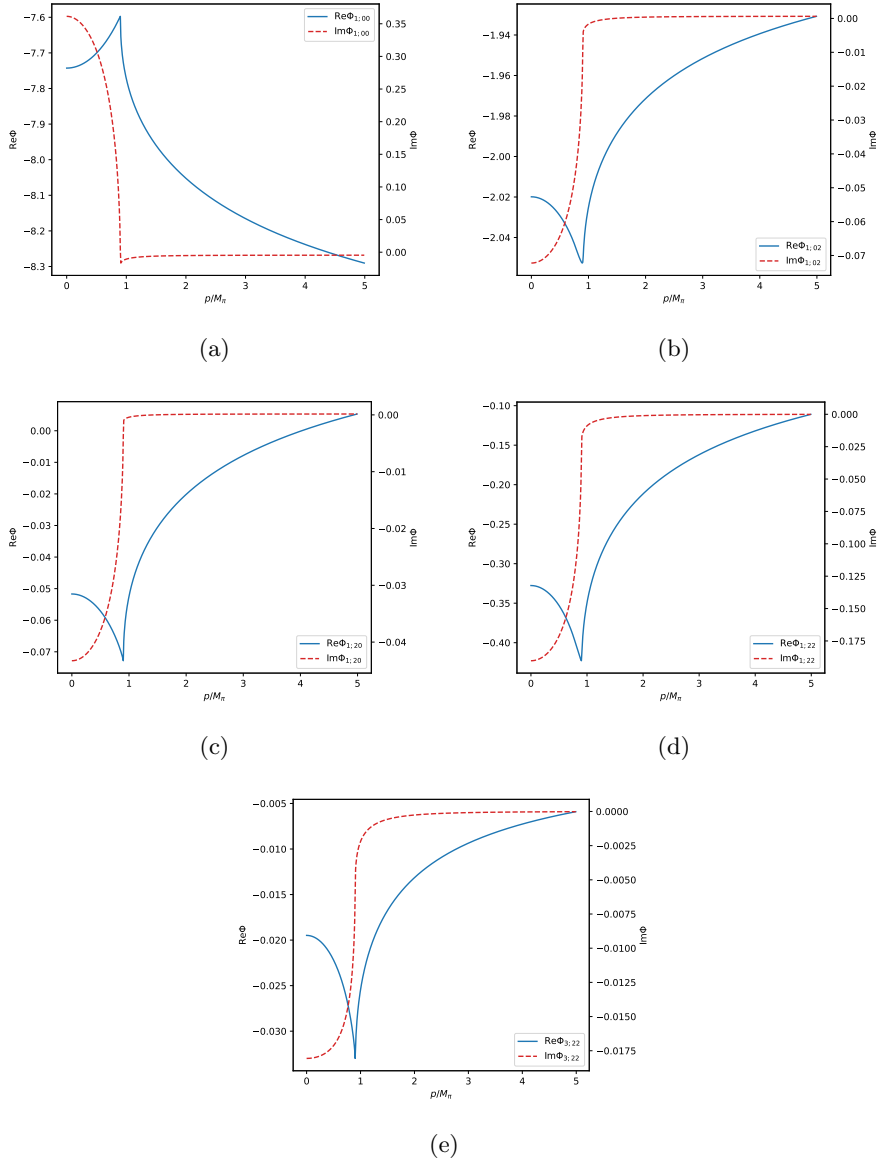


Figure 9. The solutions of Eq. (3.24), $\Phi_{1;00}$, $\Phi_{1;02}$, $\Phi_{1;20}$, $\Phi_{1;22}$ and $\Phi_{3;22}$. The blue solid line and the red dashed line represent the real and imaginary parts, respectively. The cutoff $\Lambda = 15M_\pi$ was chosen.

of the final pions. We carry our calculations at an arbitrary chosen point near the center of the Dalitz plot $m_{12}^2 = m_{23}^2 = 5M_\pi^2$.

The Fig. 13 summarizes our findings. First, Fig. 13(a) shows the calculated LL factor for different values of the cutoff $\Lambda = 15M_\pi, 20M_\pi, 25M_\pi$. The difference is hardly seen by a bare eye, confirming our expectations. Next, in Fig. 13(b), we show the results of calculations for varying three-particle threshold amplitudes by 300%, namely, for pairs (T_+^χ, T_0^χ) , and $(T_+^\chi \pm 3 \times T_+^\chi, T_0^\chi \pm 3 \times T_0^\chi)$. The cutoff is fixed at $\Lambda = 15M_\pi$. Again, the differences are small. Finally, in Fig. 13(c), we show the result of variation of scattering

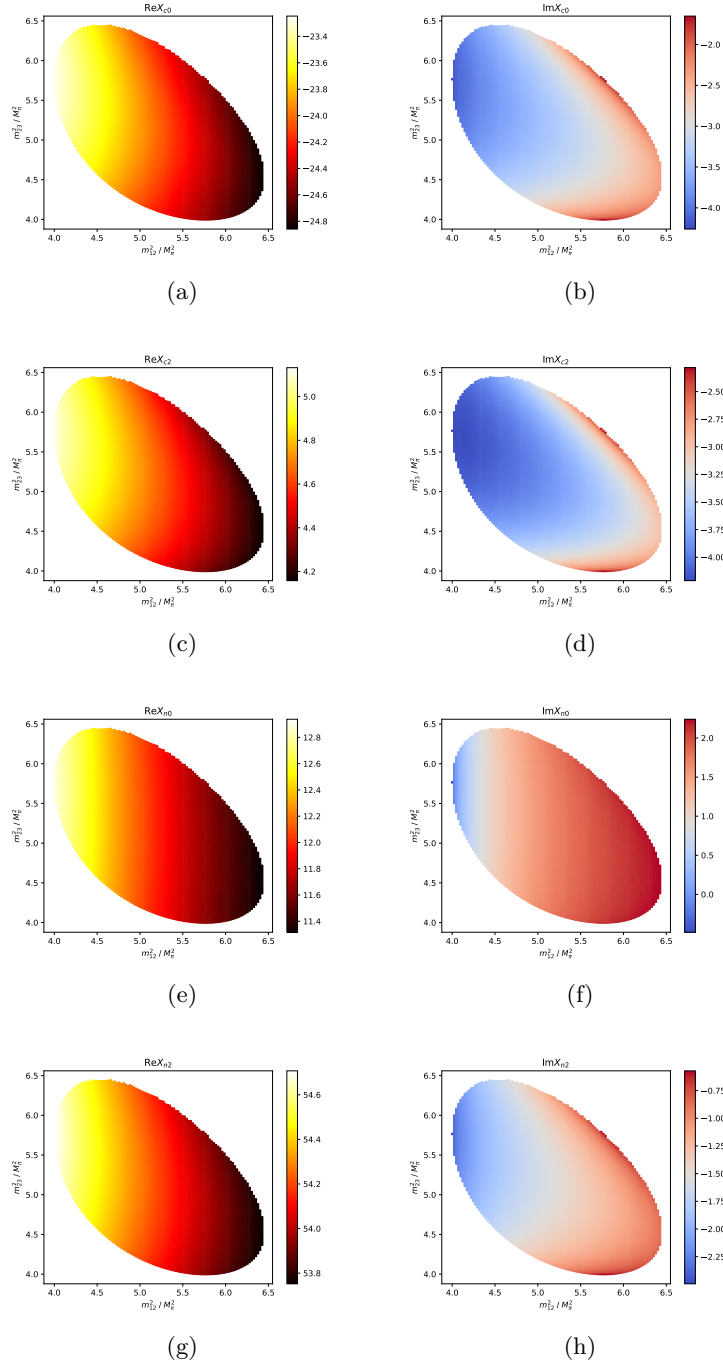


Figure 10. The real and imaginary parts of the quantities X_{c0} , X_{c2} , X_{n0} and X_{n2} in the m_{12}^2 , m_{23}^2 -plane. The cutoff $\Lambda = 15M_\pi$ is chosen.

lengths by 30% only, for the pairs (a_0, a_2) and $(a_0 \pm 0.3 \times a_0, a_2 \pm 0.3 \times a_2)$, with the three-body input (T_+^X, T_0^X) and the cutoff $\Lambda = 15M_\pi$ fixed. Now, the changes are sizable (despite the fact that the changes in the scattering lengths are factor 10 smaller than the changes in the three-body amplitudes), proving that the LL factor is much more sensitive

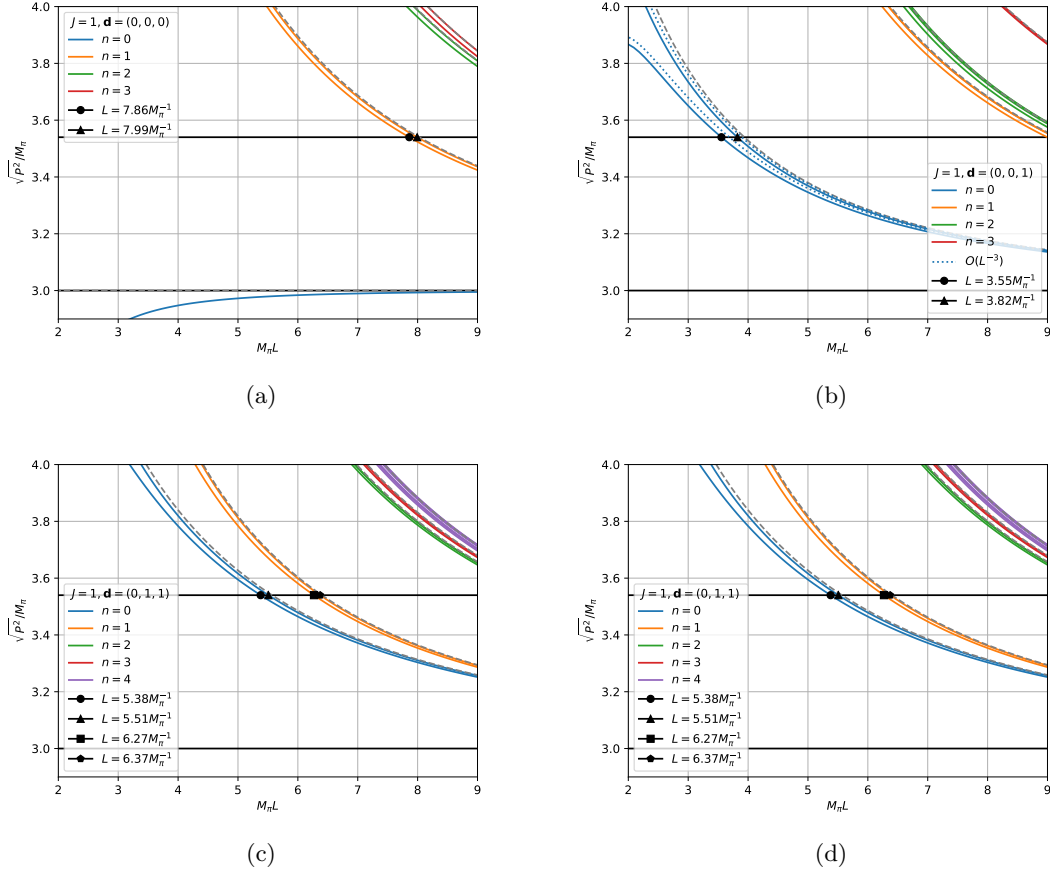


Figure 11. Finite-volume spectra of the 3π system with the total isospin $J = 3$. a) is obtained in the rest frame, irrep $\Gamma = A_1^-$. b), c), d) show the spectra in the moving frame $\mathbf{d} = (0, 0, 1)$, $\mathbf{d} = (0, 1, 1)$ and $\mathbf{d} = (1, 1, 1)$, respectively, in the irrep $\Gamma = A_2$ (the naming scheme of the irreps from Ref. [89] is used here). To compute the LL factor, we determine values of the lattice size L for which the invariant mass $\sqrt{P^2} = M_K$ (denoted by the solid black line around $\sqrt{P^2}/M_\pi \simeq 3.54$). In the subfigure b), we show perturbative energy shifts at $O(L^{-3})$ (see Eq. (C.12)). These are denoted by blue dotted lines and give a clear understanding of the fine structure of the spectrum, namely, the splitting of the unperturbed level into two levels, when the interactions are switched on.

to the two-body input than the three-body threshold amplitudes. This result constitutes the major finding of the present paper.

It is extremely important to understand the reason of such a behavior. Naively, according to the NREFT counting introduced in Sect. 2.1, the exchange term in the kernel Z and the particle-dimer coupling count as $\mathcal{O}(\delta^{-2})$ and $\mathcal{O}(1)$, respectively. This counting, however, is known not to be valid non-perturbatively [80, 81]. Namely, the particle-dimer coupling should be promoted to the leading order to cope with the singular dependence of the solutions on the cutoff. Hence, the power-counting arguments cannot directly explain a very little sensitivity of the calculated LL factor on the three-body input. In order to study this problem in more detail, we have carried out calculations for many different values of

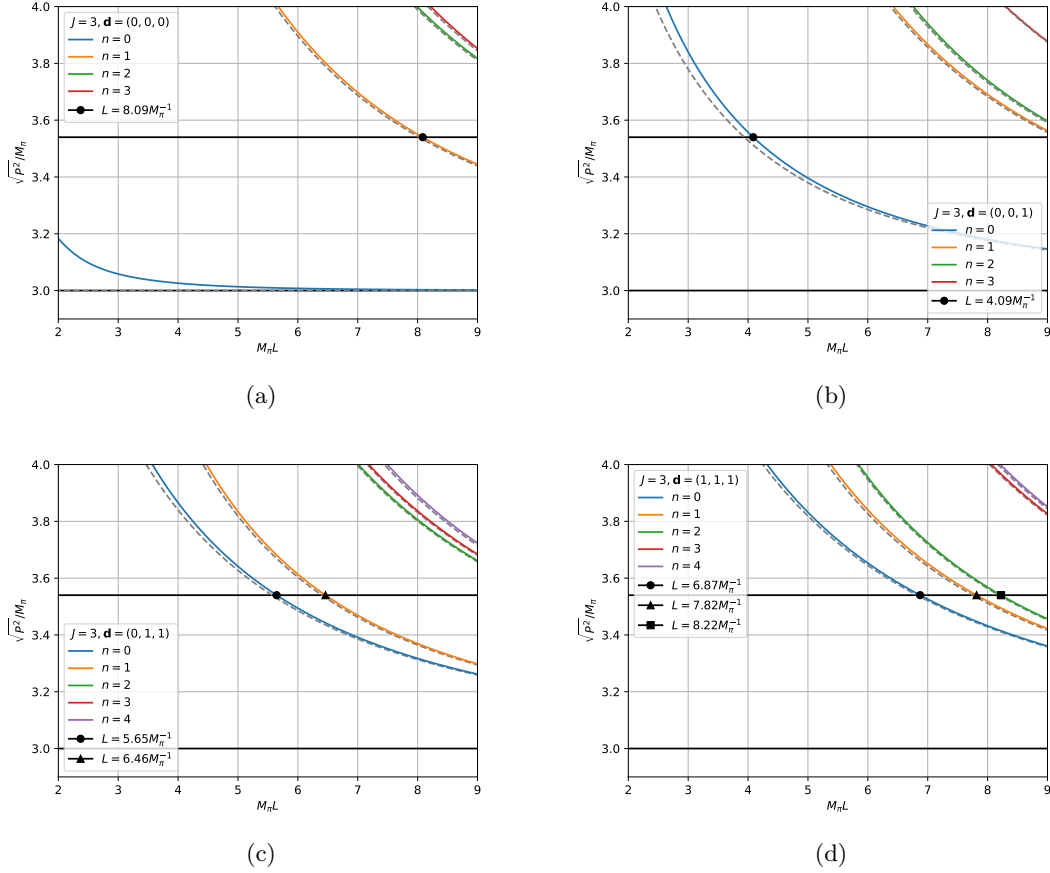


Figure 12. The same as in Fig. 11, but for the total isospin $J = 3$.

the cutoff Λ and noticed an interesting pattern: as soon as Λ came close to the critical values where the particle-dimer coupling becomes critical and flips the sign, the dependence on the three-body input grows and becomes comparable with the dependence on the values of the two-body scattering lengths, whereas away from the critical cutoffs, the dependence on the three-body input was negligible. On the basis of this observation one may argue that the formal promotion of the particle-dimer coupling to the leading order is essential in the vicinity of critical cutoffs, whereas for other values of the cutoff the arguments based on the naive counting still apply, for what concerns the numerical estimate of the relative size of different contributions. This observation also shows the importance of a proper choice of cutoff in the calculations (away from singularities), albeit the results are formally cutoff-independent.

4.4 The Weak Hamiltonian

Up to now, in the derivation of the LL factor, we did not concentrate on the weak input in the $K \rightarrow 3\pi$ decays. In other words, the couplings G_1 and G_2 are taken to be completely arbitrary. In Nature, however, these couplings are subject to further restrictions. Namely,

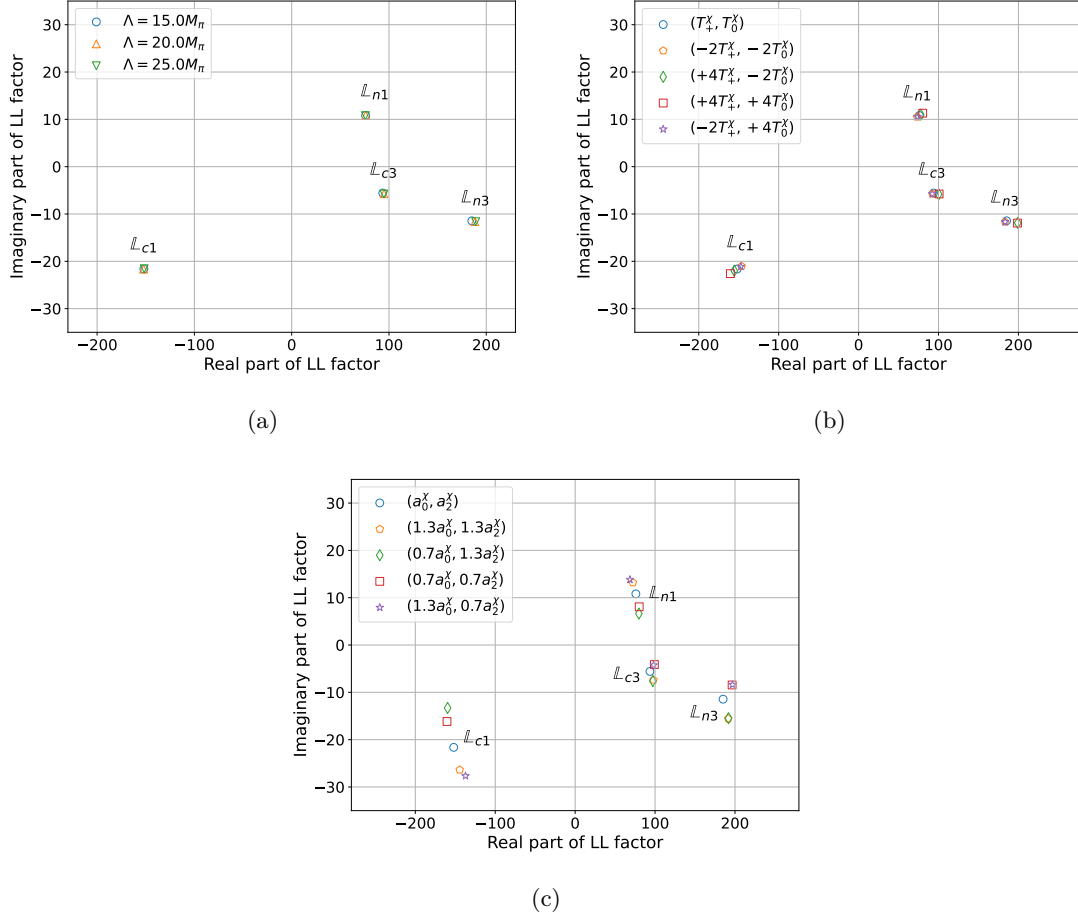


Figure 13. a) The cutoff independence of the LL factor. Here, the physical two-body scattering lengths are used and the three-body threshold amplitudes are fixed at (T_+^X, T_0^X) . The quantities \mathbb{L}_{c1} , \mathbb{L}_{c3} , \mathbb{L}_{n1} and \mathbb{L}_{n3} are obtained for three different cutoff values: $\Lambda = 15M_\pi, 20M_\pi, 25M_\pi$, represented by blue circles, brown triangles, and green inverted triangles, respectively. In b) and c), the dependence of the LL factor on the three-pion threshold amplitude and two-pion scattering lengths are illustrated.

at the lowest order in the Fermi-constant G_F , the weak decays are described by the effective weak Hamiltonian that contains $\Delta I = 1/2$ and $\Delta I = 3/2$ pieces, see e.g., [90]. Assuming conservation of isospin in strong interaction, one immediately arrives at the conclusion that the total isospin $J = 3$ decay amplitude should vanish (in real world, it is strongly suppressed by one power of G_F or isospin-breaking parameters: the fine structure constant α or $m_d - m_u$).

In order to see the consequences of this fact on the relative size of the couplings G_1 and G_2 , let us explicitly write down the vectors $|J, J_3\rangle$ with $J = 1, 2, 3$ and $J_3 = 1$ in the three-pion space:

$$|1, 1\rangle^{(1)} = \frac{1}{2} \left(|\pi^+\pi^0\pi^0\rangle - |\pi^0\pi^+\pi^0\rangle - |\pi^+\pi^-\pi^+\rangle + |\pi^-\pi^+\pi^+\rangle \right),$$

$$\begin{aligned}
|1, 1\rangle^{(2)} &= \frac{1}{\sqrt{3}} \left(|\pi^+\pi^-\pi^+\rangle - |\pi^0\pi^0\pi^+\rangle + |\pi^-\pi^+\pi^+\rangle \right), \\
|1, 1\rangle^{(3)} &= \frac{2}{\sqrt{15}} \left(6|\pi^+\pi^+\pi^-\rangle + |\pi^+\pi^-\pi^+\rangle + |\pi^-\pi^+\pi^+\rangle \right. \\
&\quad \left. - 3|\pi^0\pi^0\pi^+\rangle - 3|\pi^+\pi^0\pi^0\rangle + 2|\pi^0\pi^+\pi^0\rangle \right), \\
|2, 1\rangle^{(1)} &= \frac{1}{2} \left(|\pi^+\pi^0\pi^0\rangle - |\pi^0\pi^+\pi^0\rangle + |\pi^+\pi^-\pi^+\rangle - |\pi^-\pi^+\pi^+\rangle \right), \\
|2, 1\rangle^{(2)} &= \frac{1}{2\sqrt{3}} \left(2|\pi^+\pi^+\pi^-\rangle - |\pi^+\pi^-\pi^+\rangle - |\pi^-\pi^+\pi^+\rangle \right. \\
&\quad \left. - 2|\pi^0\pi^0\pi^+\rangle + |\pi^+\pi^0\pi^0\rangle + |\pi^0\pi^+\pi^0\rangle \right), \\
|3, 1\rangle &= \frac{1}{\sqrt{15}} \left(|\pi^+\pi^+\pi^-\rangle + |\pi^+\pi^-\pi^+\rangle + |\pi^-\pi^+\pi^+\rangle \right. \\
&\quad \left. + 2|\pi^0\pi^0\pi^+\rangle + 2|\pi^+\pi^0\pi^0\rangle + 2|\pi^0\pi^+\pi^0\rangle \right). \tag{4.17}
\end{aligned}$$

At threshold, when momenta of all particles exactly vanish, the positions of the pions in the vectors can be exchanged.¹⁶ This leads to the fact that the vectors which are antisymmetric with respect to the exchange of any pair of pions, namely, $|1, 1\rangle^{(1)}$, $|2, 1\rangle^{(1)}$ and $|2, 1\rangle^{(2)}$, vanish at threshold. From this, one can immediately conclude that the $J = 2$ amplitude does not contribute at threshold. Furthermore, it is straightforward to check that, at threshold, $|1, 1\rangle^{(2)} = \frac{\sqrt{5}}{2} |1, 1\rangle^{(3)}$. Reverting now Eq. (4.17), expressing the physical states $|\pi^0\pi^0\pi^+\rangle$ and $|\pi^+\pi^+\pi^-\rangle$ through the eigenstates of the total isospin and dropping the contributions from $J = 2, 3$, we finally arrive at a simple relation at threshold:¹⁷

$$|\pi^+\pi^+\pi^-\rangle = -2|\pi^0\pi^0\pi^+\rangle. \tag{4.18}$$

Consequently, $G_2 = -2G_1$ at leading order.

It should be pointed out that our result is in agreement with the explicit calculation of this decay amplitude at next-to-leading order in ChPT [91]. As seen from Eq. (37) of that paper, our relation exactly holds (modulo the overall sign) for the amplitudes evaluated at the center of the Dalitz plot. Furthermore, the latest fit to the experimental data by NA48 collaboration yields the value $A_+ = 1.925 \pm 0.015$ for this ratio (see Ref. [92], Eqs. (3,4)), which is quite close to our value $A_+ = 2$ (the overall sign is undefined in this analysis). The small deviation is due to the contribution of the higher-order terms in the NREFT power counting. Note finally that the difference in sign is due to the use of a particular convention for the basis states in the irreducible representations of the isospin. We consistently use Condon-Shortley phase convention in our calculations.¹⁸

In conclusion, we wish to point out that the additional restriction $G_2 = -2G_1$ does not affect our calculations of the LL factor since the latter, by definition, does not depend

¹⁶The threshold cannot be reached in physical decay process. However, one arrives at the same conclusion at the center of the Dalitz plot $m_{12}^2 = m_{23}^2 = m_{31}^2$.

¹⁷This relation directly follows from the last line in Eq. (4.17) and the symmetry of the states at threshold with respect to the permutation of the particles 1,2,3.

¹⁸Here it should be pointed out that in Eq. (2.7) of Ref. [93], which is consistent with [91], a convention different from the Condon-Shortley phase convention is used for the definition of the isospin eigenstates.

on the weak interactions that lead to the decay. The restriction simply means that only two linear combinations of $\mathbb{L}_{c1}, \mathbb{L}_{c3}, \mathbb{L}_{n1}, \mathbb{L}_{n3}$ will be needed in the final result.

5 Conclusions

Below, the results of our findings are briefly summarized:

- i) We have performed an explicit calculation of the LL factor in the $K \rightarrow 3\pi$ decays at the leading order. Albeit the general framework has been already set up [59, 60], an explicit numerical implementation of this framework is still a non-trivial exercise and represents a very useful endeavor on the way of the actual use of this framework in the analysis of the lattice QCD data. The message that we want to convey with this article, is clear: the framework for the calculation of the $K \rightarrow 3\pi$ decay amplitudes on the lattice is now ready. Moreover, higher-order terms can be systematically included in the expressions, when the accuracy of lattice data renders this inclusion necessary.
- ii) From the problems to be addressed we would like to single out the issue of the renormalization of the solutions of the Faddeev equations and the matching to the threshold three-pion amplitudes. At the first glance, the number of independent couplings that are needed to render all particle-dimer scattering amplitudes cutoff-independent, exceeds the number of three-particle threshold amplitudes at our disposal. However, as shown, the particle-dimer amplitudes that may (potentially) still have the singular cutoff dependence, do not contribute to the physical decay processes and are therefore harmless.
- iii) The main finding of the present paper is the fact that the calculated LL factor has a very weak dependence on the input three-body threshold amplitudes, even if the latter change by a factor of 3 or so. This fact has a crucial importance for the future application of this framework in the studies of kaon decays on the lattice. Namely, one may, at the first stage, avoid extracting the three-pion coupling from lattice data and use instead the rough estimate, obtained from ChPT. From our findings we conclude that even an error of 100% in the threshold amplitudes does not lead to a significant effect in the calculated LL factor, provided the cutoff Λ is chosen away from the critical values.

Acknowledgments

The authors would like to thank J. Bijnens, S. Dawid, H.-W. Hammer, B. Kubis and F. Romero-Lopez for interesting discussions. The work of R.B., F.M. and A.R. was funded in part by the Deutsche Forschungsgemeinschaft (DFG, German Research Foundation) – Project-ID 196253076 – TRR 110 and by the Ministry of Culture and Science of North Rhine-Westphalia through the NRW-FAIR project. A.R., in addition, thanks Volkswagenstiftung (grant no. 93562) and the Chinese Academy of Sciences (CAS) President’s International Fellowship Initiative (PIFI) (grant no. 2024VMB0001) for the partial financial support. The work of J.-Y.P. and J.-J.W. was supported by the National Natural

Science Foundation of China (NSFC) under Grants No. 12135011, 12175239, 12221005. The work of J.-J.W. was also supported by the National Key R&D Program of China under Contract No. 2020YFA0406400, and by Chinese Academy of Sciences under Grant No. YSBR-101.

A Integrating out the dimer fields

In order to integrate out the dimer fields, note that the dimer Lagrangian can be conveniently written as

$$\begin{aligned}\tilde{\mathcal{L}}_d &= \sum_{I,I_3} \sigma_I T_{II_3}^\dagger T_{II_3} + \sum_{I,I_3} \left(T_{II_3}^\dagger O_{II_3} + \text{h.c.} \right) \\ &+ \sum_{I,I_3,i_3} \sum_{I',I'_3,i'_3} T_{II_3}^\dagger \pi_{i_3}^\dagger h_{II_3i_3;I'I'_3i'_3} \pi_{i'_3} T_{I'I'_3} \\ &+ \sum_{I,I_3,i_3} \left(g_{II_3i_3} K_+^\dagger T_{II_3} \pi_{i_3} + \text{h.c.} \right),\end{aligned}\tag{A.1}$$

where the coefficients $h_{II_3i_3;I'I'_3i'_3}$ and $g_{II_3i_3}$ can be read off from Eq. (2.9) and Eq. (2.10) respectively – they are linear combinations of the couplings $h_j^{(I,I')}$ and $g^{(J,I)}$. Defining

$$\tilde{T}_{II_3} = \tilde{T}_{II_3} + \sum_{I'I'_3} A_{II_3;I'I'_3}^{-1} B_{I'I'_3},\tag{A.2}$$

where

$$A_{II_3;I'I'_3} = \sigma_I \delta_{II'} \delta_{I_3 I'_3} + \sum_{i_3, i'_3} \pi_{i_3}^\dagger h_{II_3i_3;I'I'_3i'_3} \pi_{i'_3},\tag{A.3}$$

and

$$B_{II_3} = O_{II_3} + \sum_{i_3} g_{II_3i_3} \pi_{i_3}^\dagger K_+, \tag{A.4}$$

the dimer Lagrangian can be brought into a quadratic form:

$$\tilde{\mathcal{L}}_d = \sum_{I,I_3} \sum_{I',I'_3} \tilde{T}_{II_3}^\dagger A_{II_3;I'I'_3} \tilde{T}_{I'I'_3} - \sum_{I,I_3} \sum_{I',I'_3} B_{II_3}^\dagger A_{II_3;I'I'_3}^{-1} B_{I'I'_3}.\tag{A.5}$$

The dimer can then be integrated out in the path integral formalism in a standard way. The second term on the right-hand side thus should be matched to the Lagrangian in the particle picture at tree level. Noting that

$$A_{II_3;I'I'_3}^{-1} = \sigma_I^{-1} \delta_{II'} \delta_{I_3 I'_3} - \sigma_I^{-1} \pi_{i_3}^\dagger h_{II_3i_3;I'I'_3i'_3} \pi_{i'_3} \sigma_{I'}^{-1} + \dots,\tag{A.6}$$

where the ellipsis contains at least four pion fields, the second term on the right hand side of Eq. (A.5) can be written as

$$- \sum_{I,I_3} \sum_{I',I'_3} B_{II_3}^\dagger A_{II_3;I'I'_3}^{-1} B_{I'I'_3} = \sum_{I,I_3} (-\sigma_I^{-1} O_{II_3}^\dagger O_{II_3})$$

$$\begin{aligned}
& + \sum_{I, I_3, i_3} \sum_{I', I'_3, i'_3} (-\sigma_I^{-1} O_{II_3}^\dagger) \pi_{i_3}^\dagger h_{II_3 i_3; I' I'_3 i'_3} \pi_{i'_3} (-\sigma_{I'}^{-1} O_{I' I'_3}) \\
& + \sum_{I, I_3, i_3} \left(g_{II_3 i_3} K_+^\dagger (-\sigma_I^{-1} O_{II_3}) \pi_{i_3} + \text{h.c.} \right) + \dots, \quad (\text{A.7})
\end{aligned}$$

where the ellipsis contains at least eight pion- or two kaon fields. These terms do not contribute to the three-body sector. We can conclude that, integrating out the dimer fields, one merely has to replace $T_{II_3} \rightarrow -\sigma_I^{-1} O_{II_3}$.

Calculating the Green function

$$G_{i'_1 i'_2 i'_3}^{II_3 i_3}(x_1, x_2, x_3) = \langle 0 | T \left[O_{3\pi}^{i'_1 i'_2 i'_3}(x_1, x_2, x_3) T_{II_3}^\dagger(0) \pi_{i_3}^\dagger(0) \right] | 0 \rangle \quad (\text{A.8})$$

in the particle-dimer picture at tree level, one performs the functional integral

$$\begin{aligned}
& \int \mathcal{D}T \mathcal{D}T^\dagger T_{II_3}^\dagger(0) \exp \left\{ -i \int d^4x \tilde{\mathcal{L}}_d \right\} \\
& = - \sum_{I' I'_3} A_{II_3; I' I'_3}^{-1} B_{I' I'_3} \exp \left\{ i \int d^4x \sum_{I', I'_3} \sum_{I'', I''_3} B_{I' I'_3}^\dagger A_{I' I'_3; I'' I''_3}^{-1} B_{I'' I''_3} \right\}. \quad (\text{A.9})
\end{aligned}$$

The remaining functional integration is over the pion and kaon fields. At tree level, only $A_{II_3; I' I'_3}^{-1} = \sigma_I^{-1} \delta_{II'} \delta_{I_3 I'_3}$ contributes and the term containing the kaon can be dropped from $B_{I' I'_3}$ in the term $A_{II_3; I' I'_3}^{-1} B_{I' I'_3}$ in front of the exponential. Thus, one may conclude that, at tree level, the above Green function in the particle picture corresponds to

$$G_{i'_1 i'_2 i'_3}^{II_3 i_3}(x_1, x_2, x_3) = \langle 0 | T \left[O_{3\pi}^{i'_1 i'_2 i'_3}(x_1, x_2, x_3) (-\sigma_I^{-1} O_{II_3}^\dagger(0)) \pi_{i_3}^\dagger(0) \right] | 0 \rangle, \quad (\text{A.10})$$

such that again the replacement $T_{II_3} \rightarrow -\sigma_I^{-1} O_{II_3}$ is justified.

Similarly, the vertex function

$$\begin{aligned}
V_{i'_1 i'_2 i'_3; j'_1 j'_2 j'_3}^{II_3 i_3; JJ_3 j_3}(x_1, x_2, x_3; y_1, y_2, y_3) & = \langle 0 | T \left[O_{3\pi}^{i'_1 i'_2 i'_3}(x_1, x_2, x_3) \left(O_{3\pi}^{j'_1 j'_2 j'_3}(y_1, y_2, y_3) \right)^\dagger \right. \\
& \quad \left. \times T_{II_3}^\dagger(0) \pi_{i_3}^\dagger(0) \pi_{j_3}(0) T_{JJ_3}(0) \right] | 0 \rangle, \quad (\text{A.11})
\end{aligned}$$

can be evaluated in the particle picture by integrating out the dimer fields. At tree level, this gives

$$\begin{aligned}
V_{i'_1 i'_2 i'_3; j'_1 j'_2 j'_3}^{II_3 i_3; JJ_3 j_3}(x_1, x_2, x_3; y_1, y_2, y_3) & = \langle 0 | T \left[O_{3\pi}^{i'_1 i'_2 i'_3}(x_1, x_2, x_3) \left(O_{3\pi}^{j'_1 j'_2 j'_3}(y_1, y_2, y_3) \right)^\dagger \right. \\
& \quad \left. \times (-\sigma_I^{-1} O_{II_3}^\dagger(0)) \pi_{i_3}^\dagger(0) \pi_{j_3}(0) (-\sigma_J^{-1} O_{JJ_3}^\dagger(0)) \right] | 0 \rangle. \quad (\text{A.12})
\end{aligned}$$

Note that, in both cases, we implicitly discard disconnected pieces in the Green functions, calculated in the particle picture.

B Three-pion amplitude in Chiral Perturbation Theory

For the matching of the particle-dimer coupling, we need to calculate the three-pion threshold amplitude in ChPT. Here, we give only a brief sketch of this calculation, carried out

at tree level, which follows the pattern outlined in Ref. [63]. In general, there are only two types of contributions, shown in Fig. 14: The contact term, which emerges from the six-pion Lagrangian, Fig. 14(a), and the exchange term that features a single pion propagator (all possible permutations of external lines in *in*- and *out*-states), Fig. 14(b). We are interested in the processes $3\pi^+ \rightarrow 3\pi^+$ and $3\pi^0 \rightarrow 3\pi^0$. The contact contributions to these processes at threshold are given by

$$\begin{aligned} T_{\text{cont}}^\chi(3\pi^+ \rightarrow 3\pi^+) &= -\frac{18M_\pi^2}{F_\pi^4}, \\ T_{\text{cont}}^\chi(3\pi^0 \rightarrow 3\pi^0) &= \frac{27M_\pi^2}{F_\pi^4}. \end{aligned} \quad (\text{B.1})$$

Symbolically, the exchange contribution can be written down as follows

$$T_{\text{ex}}^\chi(3\pi \rightarrow 3\pi) = \sum_{\text{permutations}} \mathcal{M}(2\pi \rightarrow 2\pi) \frac{1}{M_\pi^2 - k^2} \mathcal{M}(2\pi \rightarrow 2\pi), \quad (\text{B.2})$$

where k denotes the four-momentum of the exchanged pion. Furthermore, the two-body amplitudes at leading order are linear functions of the pertinent Mandelstam variables s, t, u and M_π^2 :

$$\mathcal{M}(2\pi \rightarrow 2\pi) = \frac{\alpha s + \beta t + \gamma u + \delta M_\pi^2}{F_\pi^2}. \quad (\text{B.3})$$

Here, $\alpha, \beta, \gamma, \delta$ stand for some numerical coefficients. Furthermore, one can always choose these variables so that, say, s and t depend only on the external momenta (which are, by definition, on shell). Then, one could use the relation $s + t + u = 3M_\pi^2 + k^2$ and rewrite the expression for the two-body amplitude as

$$\mathcal{M}(2\pi \rightarrow 2\pi) = \frac{\alpha s + \beta t + \gamma(4M_\pi^2 - s - t) + \gamma(k^2 - M_\pi^2) + \delta M_\pi^2}{F_\pi^2}. \quad (\text{B.4})$$

The part of the amplitude that is proportional to $k^2 - M_\pi^2$ will cancel with the propagator and will contribute to the regular part of the threshold amplitude. Separating the pole terms from the non-pole ones in all diagrams by using Eq. (B.3), in a result one gets for the regular part:

$$\begin{aligned} T_{\text{ex,reg}}^\chi(3\pi^+ \rightarrow 3\pi^+) &= \frac{36M_\pi^2}{F_\pi^4}, \\ T_{\text{ex,reg}}^\chi(3\pi^0 \rightarrow 3\pi^0) &= -\frac{225M_\pi^2}{8F_\pi^4}. \end{aligned} \quad (\text{B.5})$$

Adding up these two contributions, we finally get

$$\begin{aligned} T_{\text{reg}}^\chi(3\pi^+ \rightarrow 3\pi^+) &\doteq T_+^\chi = \frac{18M_\pi^2}{F_\pi^4}, \\ T_{\text{reg}}^\chi(3\pi^0 \rightarrow 3\pi^0) &\doteq T_0^\chi = -\frac{9M_\pi^2}{8F_\pi^4}. \end{aligned} \quad (\text{B.6})$$

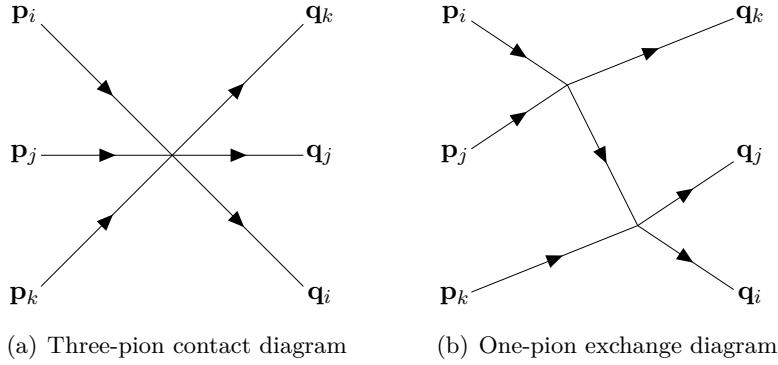


Figure 14. Two kinds of diagrams that contribute to the three-pion scattering amplitude at leading order in ChPT. Diagram (b) is singular at threshold, whereas diagram (a) is finite.

C Leading-order energy shift of the $n = 1$ state

In this appendix, we shall evaluate the energy shift of the states with the lowest energy in different moving frames as well as in the rest frame. In particular, our aim will be to demonstrate that the level splitting, which we observe in a result of the solution of the quantization condition, can be interpreted with the use of the perturbation theory as well.

We start from the states with total isospin $J = 1$ and choose $J_3 = 1$. One can define three orthogonal states with these quantum numbers [44]:

$$\begin{aligned}
|f_1\rangle &= \frac{1}{\sqrt{15}} (2|\pi^+\pi^+\pi^-\rangle + 2|\pi^+\pi^-\pi^+\rangle + 2|\pi^-\pi^+\pi^+\rangle \\
&\quad - |\pi^0\pi^0\pi^+\rangle - |\pi^0\pi^+\pi^0\rangle - |\pi^+\pi^0\pi^0\rangle), \\
|f_2\rangle &= \frac{1}{2\sqrt{3}} (2|\pi^+\pi^+\pi^-\rangle - |\pi^+\pi^-\pi^+\rangle - |\pi^-\pi^+\pi^+\rangle \\
&\quad + 2|\pi^0\pi^0\pi^+\rangle - |\pi^0\pi^+\pi^0\rangle - |\pi^+\pi^0\pi^0\rangle), \\
|f_3\rangle &= \frac{1}{2} (|\pi^+\pi^0\pi^0\rangle - |\pi^0\pi^+\pi^0\rangle - |\pi^+\pi^-\pi^+\rangle + |\pi^-\pi^+\pi^+\rangle). \tag{C.1}
\end{aligned}$$

We consider moving frames with the total three-momentum $\mathbf{P} = 2\pi\mathbf{d}/L$, where $\mathbf{d} = (0, 0, 1), (1, 1, 0), (1, 1, 1)$. For these values of \mathbf{d} , the states with the lowest energy are given by

$$|\mathbf{p}_1, \mathbf{p}_2, \mathbf{p}_3\rangle \in \{|\mathbf{P}, \mathbf{0}, \mathbf{0}\rangle, |\mathbf{0}, \mathbf{P}, \mathbf{0}\rangle, |\mathbf{0}, \mathbf{0}, \mathbf{P}\rangle\}. \tag{C.2}$$

From these we construct the total wave functions of the three-pion system denoted by

$$|f_i; \mathbf{p}_1, \mathbf{p}_2, \mathbf{p}_3\rangle, \tag{C.3}$$

where the momenta \mathbf{p}_1 , \mathbf{p}_2 and \mathbf{p}_3 are assigned to the first, second and third pion in the isospin wave function $|f_i\rangle$ respectively. Naively, in the non-interacting case there would be nine degenerate states with energy

$$E_0 = 2m + \sqrt{m^2 + \left(\frac{2\pi\mathbf{d}}{L}\right)^2}. \tag{C.4}$$

On the other hand, not all states are independent. Using Bose-symmetry we find that:

$$\begin{aligned}
|f_1; \mathbf{0}, \mathbf{P}, \mathbf{0}\rangle &= |f_1; \mathbf{P}, \mathbf{0}, \mathbf{0}\rangle, & |f_1; \mathbf{0}, \mathbf{0}, \mathbf{P}\rangle &= |f_1; \mathbf{P}, \mathbf{0}, \mathbf{0}\rangle, \\
|f_2; \mathbf{0}, \mathbf{P}, \mathbf{0}\rangle &= |f_2; \mathbf{P}, \mathbf{0}, \mathbf{0}\rangle, & |f_2; \mathbf{0}, \mathbf{0}, \mathbf{P}\rangle &= -2|f_2; \mathbf{P}, \mathbf{0}, \mathbf{0}\rangle, \\
|f_3; \mathbf{0}, \mathbf{P}, \mathbf{0}\rangle &= -|f_3; \mathbf{P}, \mathbf{0}, \mathbf{0}\rangle, & |f_3; \mathbf{0}, \mathbf{0}, \mathbf{P}\rangle &= 0, \\
|f_3; \mathbf{P}, \mathbf{0}, \mathbf{0}\rangle &= -\sqrt{3}|f_2; \mathbf{P}, \mathbf{0}, \mathbf{0}\rangle.
\end{aligned} \tag{C.5}$$

Defining the states

$$\begin{aligned}
|X; \mathbf{P}, \mathbf{0}, \mathbf{0}\rangle &= -\frac{1}{2}|f_2; \mathbf{P}, \mathbf{0}, \mathbf{0}\rangle + \frac{\sqrt{3}}{2}|f_3; \mathbf{P}, \mathbf{0}, \mathbf{0}\rangle, \\
|Y; \mathbf{P}, \mathbf{0}, \mathbf{0}\rangle &= \frac{\sqrt{3}}{2}|f_2; \mathbf{P}, \mathbf{0}, \mathbf{0}\rangle + \frac{1}{2}|f_3; \mathbf{P}, \mathbf{0}, \mathbf{0}\rangle = 0,
\end{aligned} \tag{C.6}$$

it can be seen that the lowest energy level in the frame $\mathbf{d} \neq \mathbf{0}$ with $J = 1$ is twofold degenerate, corresponding to the states $|f_1; \mathbf{P}, \mathbf{0}, \mathbf{0}\rangle$ and $|X; \mathbf{P}, \mathbf{0}, \mathbf{0}\rangle$.

The energy shift is calculated in the degenerate perturbation theory, where the potentials are obtained from the non-relativistic effective field theory. Contrary to [44], here we will use the covariant formulation. In this setup, the normalized one-particle states are given by:

$$|\pi_i(\mathbf{p})\rangle = L^{-3/2} (2w(\mathbf{p}))^{-1/2} a_i^\dagger(\mathbf{p}) |0\rangle. \tag{C.7}$$

and the creation and annihilation operators obey the commutation relation

$$[a_i(\mathbf{p}), a_j^\dagger(\mathbf{q})] = \delta_{ij} 2w(\mathbf{p}) L^3 \delta_{\mathbf{p}, \mathbf{q}}. \tag{C.8}$$

At the leading order, the energy shift $\Delta E_{\mathbf{d} \neq \mathbf{0}}^{J=1}$ is given by the eigenvalues of the potential

$$V = \frac{1}{3!} \begin{pmatrix} \langle f_1; \mathbf{P}, \mathbf{0}, \mathbf{0} | H_I | f_1; \mathbf{P}, \mathbf{0}, \mathbf{0} \rangle & \langle f_1; \mathbf{P}, \mathbf{0}, \mathbf{0} | H_I | X; \mathbf{P}, \mathbf{0}, \mathbf{0} \rangle \\ \langle X; \mathbf{P}, \mathbf{0}, \mathbf{0} | H_I | f_1; \mathbf{P}, \mathbf{0}, \mathbf{0} \rangle & \langle X; \mathbf{P}, \mathbf{0}, \mathbf{0} | H_I | X; \mathbf{P}, \mathbf{0}, \mathbf{0} \rangle \end{pmatrix}, \tag{C.9}$$

where H_I denotes the interaction Hamiltonian

$$H_I = - \int d^3\mathbf{x} \mathcal{L}_2. \tag{C.10}$$

Here \mathcal{L}_2 is the two-body Lagrangian in the particle picture, as in Eq. (2.2). The couplings C_i are matched to the $I = 0, 2$ scattering lengths a_I , according to Eq. (2.16) and Eq. (2.18).

Up to $O(L^{-3})$, the potential is given by:

$$V = \frac{4\pi}{27mL^3} \begin{pmatrix} 5(5a_0 + 4a_2) & 2\sqrt{5}(a_0 - a_2) \\ 2\sqrt{5}(a_0 - a_2) & 2(4a_0 + 5a_2) \end{pmatrix}, \tag{C.11}$$

leading to an energy shift

$$\Delta E_{\mathbf{d} \neq \mathbf{0}}^{J=1} = \frac{2\pi}{9mL^3} \left(11a_0 + 10a_2 \pm \sqrt{41a_0^2 + 20a_0a_2 + 20a_2^2} \right), \tag{C.12}$$

and lifting the degeneracy of the non-interacting energy level.

Note that the same result is obtained in the non-covariant approach. The only difference in the covariant and non-covariant potentials, besides the use of different couplings C_i , is the normalization of states: instead of the factor

$$\delta_{\mathbf{p}_i, \mathbf{q}_l} \delta_{\mathbf{p}_j + \mathbf{p}_k, \mathbf{q}_m + \mathbf{q}_n} \quad (\text{C.13})$$

which appears in Eqs. (31) and (32) of Ref. [44] for the potentials, sandwiched between the three-pion states that carry the momenta $\mathbf{p}_1, \mathbf{p}_2, \mathbf{p}_3$ and $\mathbf{q}_1, \mathbf{q}_2, \mathbf{q}_3$ respectively, in the covariant approach the following factor emerges

$$\begin{aligned} (2w(\mathbf{p}_j)2w(\mathbf{p}_k)2w(\mathbf{q}_m)2w(\mathbf{q}_n))^{-1/2} \delta_{\mathbf{p}_i, \mathbf{q}_l} \delta_{\mathbf{p}_j + \mathbf{p}_k, \mathbf{q}_m + \mathbf{q}_n} \\ = \frac{1}{4m^2} \delta_{\mathbf{p}_i, \mathbf{q}_l} \delta_{\mathbf{p}_j + \mathbf{p}_k, \mathbf{q}_m + \mathbf{q}_n} + \dots \end{aligned} \quad (\text{C.14})$$

Here the multiplicative factors $2w(\mathbf{k}_i)$ account for the different normalization of the one-particle states in the relativistic and non-relativistic framework, see Eq. (C.7). For the same reason, these factors also arise in the matching condition in the non-covariant framework, while in the covariant matching condition they are absent. Therefore the results after expressing everything in terms of the scattering lengths are identical.

Next, note that, for $J = 3$, there is only a single state with the lowest energy. One can, for example, choose $J_3 = 3$ and consider the state $|\pi^+ \pi^+ \pi^+; \mathbf{P}, \mathbf{0}, \mathbf{0}\rangle$. The energy shift at the leading order can be calculated in the non-degenerate perturbation theory and is given by

$$\Delta E_{\mathbf{d} \neq \mathbf{0}}^{J=3} = \frac{1}{3!} \langle \pi^+ \pi^+ \pi^+; \mathbf{P}, \mathbf{0}, \mathbf{0} | H_I | \pi^+ \pi^+ \pi^+; \mathbf{P}, \mathbf{0}, \mathbf{0} \rangle = \frac{20\pi}{3mL^3} a_2. \quad (\text{C.15})$$

Finally, note that for the ground state $\mathbf{d} = \mathbf{0}$, the energy shifts corresponding to the total isospin $J = 1$ and $J = 3$ can be obtained in the non-degenerate perturbation theory again. For $J = 1$ and $J_3 = 1$, only the state $|f_1; \mathbf{0}, \mathbf{0}, \mathbf{0}\rangle$ yields the non-vanishing ground-state wave function due to Bose-symmetry. The energy shift is then given by:

$$\Delta E_{\mathbf{d}=\mathbf{0}}^{J=1} = \frac{4\pi}{3mL^3} (5a_0 + 4a_2). \quad (\text{C.16})$$

For $J = 3$ and $J_3 = 3$, the ground-state wave function is given by $|\pi^+ \pi^+ \pi^+; \mathbf{0}, \mathbf{0}, \mathbf{0}\rangle$. At the leading order, the energy shift of this state is equal to

$$\Delta E_{\mathbf{d}=\mathbf{0}}^{J=3} = \frac{12\pi}{mL^3} a_2. \quad (\text{C.17})$$

References

- [1] Maxwell T. Hansen and Stephen R. Sharpe. Relativistic, model-independent, three-particle quantization condition. *Phys. Rev.*, D90(11):116003, 2014.
- [2] Maxwell T. Hansen and Stephen R. Sharpe. Expressing the three-particle finite-volume spectrum in terms of the three-to-three scattering amplitude. *Phys. Rev.*, D92(11):114509, 2015.

- [3] Hans-Werner Hammer, Jin-Yi Pang, and A. Rusetsky. Three-particle quantization condition in a finite volume: 1. The role of the three-particle force. *JHEP*, 09:109, 2017.
- [4] H. W. Hammer, J. Y. Pang, and A. Rusetsky. Three particle quantization condition in a finite volume: 2. General formalism and the analysis of data. *JHEP*, 10:115, 2017.
- [5] M. Mai and M. Döring. Three-body Unitarity in the Finite Volume. *Eur. Phys. J.*, A53(12):240, 2017.
- [6] Maxim Mai and Michael Döring. Finite-Volume Spectrum of $\pi^+\pi^+$ and $\pi^+\pi^+\pi^+$ Systems. *Phys. Rev. Lett.*, 122(6):062503, 2019.
- [7] Simon Kreuzer and H. W. Hammer. Efimov physics in a finite volume. *Phys. Lett. B*, 673:260–263, 2009.
- [8] Simon Kreuzer and H. W. Hammer. On the modification of the Efimov spectrum in a finite cubic box. *Eur. Phys. J. A*, 43:229–240, 2010.
- [9] Simon Kreuzer and H. W. Hammer. The triton in a finite volume. *Phys. Lett. B*, 694:424–429, 2011.
- [10] Simon Kreuzer and Harald W. Griebhammer. Three particles in a finite volume: The breakdown of spherical symmetry. *Eur. Phys. J. A*, 48:93, 2012.
- [11] Raúl A. Briceño and Zohreh Davoudi. Three-particle scattering amplitudes from a finite volume formalism. *Phys. Rev.*, D87(9):094507, 2013.
- [12] K. Polejaeva and A. Rusetsky. Three particles in a finite volume. *Eur. Phys. J. A*, 48:67, 2012.
- [13] M. Jansen, H. W. Hammer, and Yu Jia. Finite volume corrections to the binding energy of the X(3872). *Phys. Rev. D*, 92(11):114031, 2015.
- [14] Maxwell T. Hansen and Stephen R. Sharpe. Perturbative results for two and three particle threshold energies in finite volume. *Phys. Rev.*, D93:014506, 2016.
- [15] Maxwell T. Hansen and Stephen R. Sharpe. Threshold expansion of the three-particle quantization condition. *Phys. Rev.*, D93(9):096006, 2016. [Erratum: *Phys. Rev.* **D96**, 039901 (2017)].
- [16] Peng Guo. One spatial dimensional finite volume three-body interaction for a short-range potential. *Phys. Rev.*, D95(5):054508, 2017.
- [17] Stephen R. Sharpe. Testing the threshold expansion for three-particle energies at fourth order in ϕ^4 theory. *Phys. Rev.*, D96(5):054515, 2017.
- [18] Peng Guo and Vladimir Gasparian. Numerical approach for finite volume three-body interaction. *Phys. Rev. D*, 97(1):014504, 2018.
- [19] Peng Guo and Vladimir Gasparian. A solvable three-body model in finite volume. *Phys. Lett.*, B774:441–445, 2017.
- [20] Yu Meng, Chuan Liu, Ulf-G Meißner, and A. Rusetsky. Three-particle bound states in a finite volume: unequal masses and higher partial waves. *Phys. Rev. D*, 98(1):014508, 2018.
- [21] R. A. Briceño, Maxwell T. Hansen, and Stephen R. Sharpe. Relating the finite-volume spectrum and the two-and-three-particle S matrix for relativistic systems of identical scalar particles. *Phys. Rev.*, D95(7):074510, 2017.

- [22] Peng Guo, Michael Döring, and Adam P. Szczepaniak. Variational approach to N -body interactions in finite volume. *Phys. Rev.*, D98(9):094502, 2018.
- [23] Peng Guo and Tyler Morris. Multiple-particle interaction in (1+1)-dimensional lattice model. *Phys. Rev. D*, 99(1):014501, 2019.
- [24] P. Klos, S. König, H. W. Hammer, J. E. Lynn, and A. Schwenk. Signatures of few-body resonances in finite volume. *Phys. Rev.*, C98(3):034004, 2018.
- [25] Raúl A. Briceño, Maxwell T. Hansen, and Stephen R. Sharpe. Numerical study of the relativistic three-body quantization condition in the isotropic approximation. *Phys. Rev.*, D98(1):014506, 2018.
- [26] Raúl A. Briceño, Maxwell T. Hansen, and Stephen R. Sharpe. Three-particle systems with resonant subprocesses in a finite volume. *Phys. Rev.*, D99(1):014516, 2019.
- [27] M. Mai, M. Döring, C. Culver, and A. Alexandru. Three-body unitarity versus finite-volume $\pi^+\pi^+\pi^+$ spectrum from lattice QCD. *Phys. Rev. D*, 101:054510, 2020.
- [28] Peng Guo and Michael Döring. Lattice model of heavy-light three-body system. *Phys. Rev. D*, 101(3):034501, 2020.
- [29] Peng Guo. Modeling few-body resonances in finite volume. *Phys. Rev. D*, 102(5):054514, 2020.
- [30] Tyler D. Blanton, Fernando Romero-López, and Stephen R. Sharpe. Implementing the three-particle quantization condition including higher partial waves. *JHEP*, 03:106, 2019.
- [31] Jin-Yi Pang, Jia-Jun Wu, H. W. Hammer, Ulf-G. Meißner, and Akaki Rusetsky. Energy shift of the three-particle system in a finite volume. *Phys. Rev.*, D99(7):074513, 2019.
- [32] A. W. Jackura, S. M. Dawid, C. Fernández-Ramírez, V. Mathieu, M. Mikhasenko, A. Pilloni, S. R. Sharpe, and A. P. Szczepaniak. Equivalence of three-particle scattering formalisms. *Phys. Rev. D*, 100(3):034508, 2019.
- [33] Raúl A. Briceño, Maxwell T. Hansen, Stephen R. Sharpe, and Adam P. Szczepaniak. Unitarity of the infinite-volume three-particle scattering amplitude arising from a finite-volume formalism. *Phys. Rev.*, D100(5):054508, 2019.
- [34] Fernando Romero-López, Stephen R. Sharpe, Tyler D. Blanton, Raúl A. Briceño, and Maxwell T. Hansen. Numerical exploration of three relativistic particles in a finite volume including two-particle resonances and bound states. *JHEP*, 10:007, 2019.
- [35] Sebastian König. Few-body bound states and resonances in finite volume. *Few Body Syst.*, 61(3):20, 2020.
- [36] Ruairí Brett, Chris Culver, Maxim Mai, Andrei Alexandru, Michael Döring, and Frank X. Lee. Three-body interactions from the finite-volume QCD spectrum. *Phys. Rev. D*, 104(1):014501, 2021.
- [37] Maxwell T. Hansen, Fernando Romero-López, and Stephen R. Sharpe. Generalizing the relativistic quantization condition to include all three-pion isospin channels. *JHEP*, 07:047, 2020.
- [38] Tyler D. Blanton and Stephen R. Sharpe. Alternative derivation of the relativistic three-particle quantization condition. *Phys. Rev. D*, 102(5):054520, 2020.
- [39] Tyler D. Blanton and Stephen R. Sharpe. Equivalence of relativistic three-particle quantization conditions. *Phys. Rev. D*, 102(5):054515, 2020.

- [40] Jin-Yi Pang, Jia-Jun Wu, and Li-Sheng Geng. *DDK* system in finite volume. *Phys. Rev. D*, 102(11):114515, 2020.
- [41] Maxwell T. Hansen, Raúl A. Briceño, Robert G. Edwards, Christopher E. Thomas, and David J. Wilson. Energy-Dependent $\pi^+\pi^+\pi^+$ Scattering Amplitude from QCD. *Phys. Rev. Lett.*, 126:012001, 2021.
- [42] Fernando Romero-López, Akaki Rusetsky, Nikolas Schlage, and Carsten Urbach. Relativistic N -particle energy shift in finite volume. *JHEP*, 02:060, 2021.
- [43] Tyler D. Blanton and Stephen R. Sharpe. Relativistic three-particle quantization condition for nondegenerate scalars. *Phys. Rev. D*, 103(5):054503, 2021.
- [44] Fabian Müller, Akaki Rusetsky, and Tiansu Yu. Finite-volume energy shift of the three-pion ground state. *Phys. Rev. D*, 103(5):054506, 2021.
- [45] Tyler D. Blanton and Stephen R. Sharpe. Three-particle finite-volume formalism for $\pi^+\pi^+K^+$ and related systems. *Phys. Rev. D*, 104(3):034509, 2021.
- [46] Fabian Müller, Jin-Yi Pang, Akaki Rusetsky, and Jia-Jun Wu. Relativistic-invariant formulation of the NREFT three-particle quantization condition. *JHEP*, 02:158, 2022.
- [47] Silas R. Beane, William Detmold, Thomas C. Luu, Kostas Orginos, Martin J. Savage, and Aaron Torok. Multi-Pion Systems in Lattice QCD and the Three-Pion Interaction. *Phys. Rev. Lett.*, 100:082004, 2008.
- [48] William Detmold, Martin J. Savage, Aaron Torok, Silas R. Beane, Thomas C. Luu, Kostas Orginos, and Assumpta Parreno. Multi-Pion States in Lattice QCD and the Charged-Pion Condensate. *Phys. Rev.*, D78:014507, 2008.
- [49] William Detmold, Kostas Orginos, Martin J. Savage, and Andre Walker-Loud. Kaon Condensation with Lattice QCD. *Phys. Rev. D*, 78:054514, 2008.
- [50] Tyler D. Blanton, Fernando Romero-López, and Stephen R. Sharpe. $I = 3$ three-pion scattering amplitude from lattice QCD. *Phys. Rev. Lett.*, 124(3):032001, 2020.
- [51] Ben Hörz and Andrew Hanlon. Two- and three-pion finite-volume spectra at maximal isospin from lattice QCD. *Phys. Rev. Lett.*, 123(14):142002, 2019.
- [52] Chris Culver, Maxim Mai, Ruairí Brett, Andrei Alexandru, and Michael Döring. Three pion spectrum in the $I = 3$ channel from lattice QCD. *Phys. Rev. D*, 101(11):114507, 2020.
- [53] Matthias Fischer, Bartosz Kostrzewa, Liuming Liu, Fernando Romero-López, Martin Ueding, and Carsten Urbach. Scattering of two and three physical pions at maximal isospin from lattice QCD. *Eur. Phys. J. C*, 81(5):436, 2021.
- [54] Andrei Alexandru, Ruairí Brett, Chris Culver, Michael Döring, Dehua Guo, Frank X. Lee, and Maxim Mai. Finite-volume energy spectrum of the $K^-K^-K^-$ system. *Phys. Rev. D*, 102(11):114523, 2020.
- [55] Fernando Romero-López, Akaki Rusetsky, and Carsten Urbach. Two- and three-body interactions in φ^4 theory from lattice simulations. *Eur. Phys. J.*, C78(10):846, 2018.
- [56] Tyler D. Blanton, Andrew D. Hanlon, Ben Hörz, Colin Morningstar, Fernando Romero-López, and Stephen R. Sharpe. Interactions of two and three mesons including higher partial waves from lattice QCD. *JHEP*, 10:023, 2021.
- [57] Maxim Mai, Andrei Alexandru, Ruairí Brett, Chris Culver, Michael Döring, Frank X. Lee,

- and Daniel Sadasivan. Three-Body Dynamics of the $a_1(1260)$ Resonance from Lattice QCD. *Phys. Rev. Lett.*, 127(22):222001, 2021.
- [58] Fabian Müller and Akaki Rusetsky. On the three-particle analog of the Lellouch-Lüscher formula. *JHEP*, 03:152, 2021.
- [59] Fabian Müller, Jin-Yi Pang, Akaki Rusetsky, and Jia-Jun Wu. Three-particle Lellouch-Lüscher formalism in moving frames. *JHEP*, 02:214, 2023.
- [60] Maxwell T. Hansen, Fernando Romero-López, and Stephen R. Sharpe. Decay amplitudes to three hadrons from finite-volume matrix elements. *JHEP*, 04:113, 2021.
- [61] Tyler D. Blanton, Fernando Romero-López, and Stephen R. Sharpe. Implementing the three-particle quantization condition for $\pi^+\pi^+K^+$ and related systems. *JHEP*, 02:098, 2022.
- [62] Daniel Severt, Maxim Mai, and Ulf-G. Meißner. Particle-dimer approach for the Roper resonance in a finite volume. *JHEP*, 04:100, 2023.
- [63] Jorge Baeza-Ballesteros, Johan Bijnens, Tomáš Husek, Fernando Romero-López, Stephen R. Sharpe, and Mattias Sjö. The isospin-3 three-particle K-matrix at NLO in ChPT. *JHEP*, 05:187, 2023.
- [64] Zachary T. Draper, Maxwell T. Hansen, Fernando Romero-López, and Stephen R. Sharpe. Three relativistic neutrons in a finite volume. *JHEP*, 07:226, 2023.
- [65] Rishabh Bubna, Fabian Müller, and Akaki Rusetsky. Finite-volume energy shift of the three-nucleon ground state. *Phys. Rev. D*, 108(1):014518, 2023.
- [66] Maxwell T. Hansen and Stephen R. Sharpe. Lattice QCD and Three-particle Decays of Resonances. *Ann. Rev. Nucl. Part. Sci.*, 69:65–107, 2019.
- [67] Maxim Mai, Michael Döring, and Akaki Rusetsky. Multi-particle systems on the lattice and chiral extrapolations: a brief review. *Eur. Phys. J. ST*, 230(6):1623–1643, 2021.
- [68] Laurent Lellouch and Martin Luscher. Weak transition matrix elements from finite volume correlation functions. *Commun. Math. Phys.*, 219:31–44, 2001.
- [69] Toby Peterken and Maxwell T. Hansen. Higher partial wave contamination in finite-volume 1-to-2 transitions. 4 2023.
- [70] Harvey B. Meyer. Lattice QCD and the Timelike Pion Form Factor. *Phys. Rev. Lett.*, 107:072002, 2011.
- [71] Maxwell T. Hansen and Stephen R. Sharpe. Multiple-channel generalization of Lellouch-Luscher formula. *Phys. Rev. D*, 86:016007, 2012.
- [72] V. Bernard, D. Hoja, U. G. Meißner, and A. Rusetsky. Matrix elements of unstable states. *JHEP*, 09:023, 2012.
- [73] Vincenzo Cirigliano, Gerhard Ecker, Helmut Neufeld, Antonio Pich, and Jorge Portoles. Kaon Decays in the Standard Model. *Rev. Mod. Phys.*, 84:399, 2012.
- [74] J. R. Batley et al. Search for direct CP violating charge asymmetries in $K^{*+} \rightarrow \pi^{*+} \pi^+ \pi^-$ and $K^{*+} \rightarrow \pi^{*+} \pi^0 \pi^0$ decays. *Eur. Phys. J. C*, 52:875–891, 2007.
- [75] Gilberto Colangelo, Juerg Gasser, Bastian Kubis, and Akaki Rusetsky. Cusps in $K \rightarrow 3\pi$ decays. *Phys. Lett. B*, 638:187–194, 2006.
- [76] Jurg Gasser, Bastian Kubis, and Akaki Rusetsky. Cusps in $K \rightarrow 3\pi$ decays: a theoretical framework. *Nucl. Phys. B*, 850:96–147, 2011.

- [77] M. Ebert, H. W. Hammer, and A. Rusetsky. An alternative scheme for effective range corrections in pionless EFT. *Eur. Phys. J. A*, 57(12):332, 2021.
- [78] Jin-Yi Pang, Martin Ebert, Hans-Werner Hammer, Fabian Müller, Akaki Rusetsky, and Jia-Jun Wu. Spurious poles in a finite volume. *JHEP*, 07:019, 2022.
- [79] M. Ebert, H. W. Hammer, and A. Rusetsky. An Alternative Scheme for Pionless EFT: Neutron-Deuteron Scattering in the Doublet S-Wave. *Few Body Syst.*, 64(4):87, 2023.
- [80] Paulo F. Bedaque, H. W. Hammer, and U. van Kolck. Renormalization of the three-body system with short range interactions. *Phys. Rev. Lett.*, 82:463–467, 1999.
- [81] Paulo F. Bedaque, H. W. Hammer, and U. van Kolck. The Three boson system with short range interactions. *Nucl. Phys. A*, 646:444–466, 1999.
- [82] Paulo F. Bedaque, H. W. Hammer, and U. van Kolck. Effective theory for neutron deuteron scattering: Energy dependence. *Phys. Rev. C*, 58:R641–R644, 1998.
- [83] M. Döring, H. W. Hammer, M. Mai, J. Y. Pang, A. Rusetsky, and J. Wu. Three-body spectrum in a finite volume: the role of cubic symmetry. *Phys. Rev. D*, 97(11):114508, 2018.
- [84] W. Glockle. S-matrix pole trajectory in a three-neutron model. *Phys. Rev. C*, 18:564–572, 1978.
- [85] R. T. Cahill and I. H. Sloan. Theory of neutron-deuteron break-up at 14.4 MeV. *Nucl. Phys. A*, 165:161–179, 1971. [Erratum: *Nucl.Phys.A* 196, 632–632 (1972)].
- [86] Marco Garofalo, Maxim Mai, Fernando Romero-López, Akaki Rusetsky, and Carsten Urbach. Three-body resonances in the φ^4 theory. *JHEP*, 02:252, 2023.
- [87] Sebastian M. Dawid, Md Habib E. Islam, and Raúl A. Briceño. Analytic continuation of the relativistic three-particle scattering amplitudes. *Phys. Rev. D*, 108(3):034016, 2023.
- [88] Erich W. Schmid and Horst Ziegelmann. *Quantum Mechanical Three-body Problem*. Vieweg, 12 1974.
- [89] M. Göckeler, R. Horsley, M. Lage, U. G. Meißner, P. E. L. Rakow, A. Rusetsky, G. Schierholz, and J. M. Zanotti. Scattering phases for meson and baryon resonances on general moving-frame lattices. *Phys. Rev. D*, 86:094513, 2012.
- [90] Gerhard Buchalla, Andrzej J. Buras, and Markus E. Lautenbacher. Weak decays beyond leading logarithms. *Rev. Mod. Phys.*, 68:1125–1144, 1996.
- [91] Johan Bijnens, Pierre Dhonte, and Fredrik Borg. $K \rightarrow 3\pi$ decays in chiral perturbation theory. *Nucl. Phys. B*, 648:317–344, 2003.
- [92] J. R. Batley et al. Determination of the S-wave $\pi\pi$ scattering lengths from a study of $K^+ \rightarrow \pi^+\pi^0\pi^0$ decays. *Eur. Phys. J. C*, 64:589–608, 2009.
- [93] Charles Zemah. Three-pion decays of unstable particles. *Phys. Rev. B*, 133:1201, 1964.